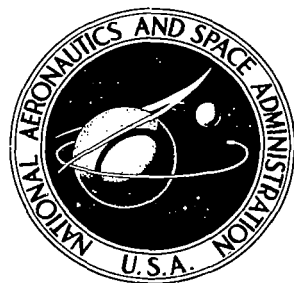


# NASA CONTRACTOR REPORT

NASA CR-2068



NASA CR-2068

2.1



LOAN COPY: RETURN TO  
AFWL (DOUL)  
KIRTLAND AFB, N. M.

## COMPUTER PROGRAM FOR CALCULATING LAMINAR AND TURBULENT BOUNDARY LAYER DEVELOPMENT IN COMPRESSIBLE FLOW

*by H. J. Herring and G. L. Mellor*

*Prepared by*  
PRINCETON UNIVERSITY  
Princeton, N.J.  
*for Lewis Research Center*





0061224

1. Report No. NASA CR-2068	2. Government Accession No.	3. Recipient's Catalog No.	
4. Title and Subtitle COMPUTER PROGRAM FOR CALCULATING LAMINAR AND TURBULENT BOUNDARY LAYER DEVELOPMENT IN COMPRESSIBLE FLOW		5. Report Date June 1972	6. Performing Organization Code
		8. Performing Organization Report No. None	10. Work Unit No.
7. Author(s) H. J. Herring and G. L. Mellor		11. Contract or Grant No. NGR 31-001-074	
		13. Type of Report and Period Covered Contractor Report	
9. Performing Organization Name and Address Princeton University Princeton, New Jersey		14. Sponsoring Agency Code	
		12. Sponsoring Agency Name and Address National Aeronautics and Space Administration Washington, D.C. 20546	
15. Supplementary Notes Project Managers, S. Lieblein and A. V. Saule, V/STOL and Noise Division, NASA Lewis Research Center, Cleveland, Ohio			
16. Abstract This report describes a computer program which performs a numerical integration of the equations of motion for a compressible two-dimensional boundary layer. Boundary layer calculations may be carried out for both laminar and turbulent flow for arbitrary Reynolds number and freestream Mach number distribution on planar or axisymmetric bodies with wall heating or cooling, longitudinal wall curvature, wall suction or blowing, and a rough or a smooth wall. A variety of options are available as initial conditions. The program can generate laminar initial conditions such as Falkner-Skan similarity solutions (so that initial wedge flows can be simulated including Blasius or stagnation point flow) or approximate equilibrium turbulent profiles. Alternatively, initial profile input data can be utilized.			
17. Key Words (Suggested by Author(s)) Boundary layer Compressible flow Computer program		18. Distribution Statement Unclassified - unlimited	
19. Security Classif. (of this report) Unclassified	20. Security Classif. (of this page) Unclassified	21. No. of Pages 94	22. Price* \$3.00



## TABLE OF CONTENTS

I.	INTRODUCTION	1
II.	ANALYTICAL FUNDAMENTALS	4
	Equations of Motion	4
	Initialization	14
	Approximate laminar similarity flow	15
	Approximate turbulent similarity flow	18
III.	NUMERICAL METHOD	23
	Reduction to Ordinary Differential Equations	23
	Solution of Ordinary Differential Equations	28
IV.	COMPUTER PROGRAM	32
	Program Notation	32
	Main Program	40
	Description of the Subroutines	55
V.	PROGRAM OPERATION	61
	Input	61
	Output	70
	Illustrative Examples	72
	Identification of Malfunctions	72
	REFERENCES	86

## NOTATION

The number in curved brackets following some of the notational definitions is the number of the equation in the text which defines the variable. The quantity in square brackets is the equivalent notation used in the computer program.

$A(\beta)$	Parameter in skin friction equation (II-33).
$A_h(\beta)$	Parameter in Stanton number equation (II-36).
$a_{m_j}$	Variables used in the Gaussian elimination method (III-16), [AM], $m = 1, 4$ .
$B$	Exponent in expression for freestream velocity variation in laminar similarity solution (II-28), [BS].
$B_h$	Parameter in Stanton number equation (II-36).
$B_s$	Parameter in skin friction equation (II-33).
$b_1 \dots b_5$	Coefficients in equations (III-7,8), [B].
$C$	Constant of proportionality in expression for $\delta^*$ in laminar similarity solution (II-28), [C].
$C_a =$	$2(\delta^*/r_w) \cos \alpha$ , parameter related to axisymmetric flow appearing in equation (II-14), [CA].
$C_f =$	$\tau_w/(\rho_e U^2/2)$ , coefficient of skin friction, [CF].
$C_p$	Specific heat at constant pressure.
$C_u =$	$(\delta^*/c_w)(u/U)/[(\partial(u/U)/\partial\eta)]$ , longitudinal curvature parameter in equation (IV-2), [CU].
$C_\mu$	Parameter in skin friction relation (II-34), [CMU].
$c_w$	Radius of longitudinal curvature in the same unit as $x$ , [CW].
$c_0 \dots c_8$	Coefficients in equations (III-4) and (III-5), [CO...C8].
$d$	$\rho_e/\rho$ , density ratio, [D].

- $f'$  =  $(\rho_e U - \rho u) / \rho_e U$ , velocity defect variable, [FP].
- $\hat{f}'$  Transformed independent variable defined by equation (III-3).
- $g'$  =  $(h_e^\circ - h^\circ) / (h_e^\circ - h_r)$ , enthalpy defect variable, [GP].
- $H$  =  $(h_e^\circ - h_r) / h_e^\circ$ , [BH].
- $h$  Static enthalpy.
- $h_r$  Arbitrary reference enthalpy.
- $h^\circ$  =  $h + u^2/2$ , total enthalpy.
- $i, j$  Indices of variables in the  $x$  and  $y$  directions respectively, [I, J].
- $k$  = Specific heat ratio, [SHR].
- $L$  =  $x_2 - x_1$ , position at which  $R_L$  is defined in laminar similarity (II-28).
- $M_e$  = Freestream Mach number, [M].
- $P$  =  $\delta^* U_x / U$ , parameter in equation (II-14), [P].
- $P^*$  =  $R_{\delta^*} P$ , parameter in laminar similarity flow, [P].
- $P_r$  =  $v/v_g$ , Prandtl number, [PR].
- $P_{rt}$  =  $(v_e - v) / (v_{eg} - v_g)$ , turbulent Prandtl number, [PRT].
- $Q$  =  $(\rho_e U \delta^*)_x / \rho_e U$ , parameter in equation (II-14), [Q].
- $Q^*$  =  $R_{\delta^*} Q$ , parameter in laminar similarity flow, [Q].
- $q$  Local heat flux (II-4b).
- $R$  =  $r_{w_x} \delta^* / r_w$ , [R].
- $R^*$  =  $R_{\delta^*} R$ , parameter in laminar similarity flow, [R].
- $R_L$  =  $(x_2 - x_1) U / \nu$ , Reynolds number in laminar similarity solution, [RL].

$R_{\delta^*}$	=	$\delta^*U/\nu$ , Reynolds number based on displacement thickness, [RDT].
$r$	=	$r_w(\bar{x}) + \bar{y} \cos \alpha(\bar{x})$ , radius of a point in the boundary layer in the same units as $x$ .
$r_w$		Radius of surface in the same units as $x$ , [RW].
$S_c$		Sutherland constant (II-18), [STC].
$S_t$	=	$q_w/[\rho_e U(h_e^o - h_w)]$ , Stanton number, [ST].
$S_{tr}$	=	$q_w/[\rho_e U(h_e^o - h_r)]$ , reference Stanton number, [STR].
$s_w$		Characteristic size of roughness elements in the same units as $x$ , [SW].
$T$		Proportion of turbulence viscosity in effective viscosity, (IV-4), [TURB].
$U$		Freestream velocity; arbitrary dimensional units, [U].
$U_L$		Freestream velocity at $x_2$ in laminar similarity solution in the same units as $U$ , [U(2)].
$u, v$		Time average velocities in the $x$ and $y$ directions respectively.
$u_\tau$	=	$\sqrt{\tau_w/\rho_w}$ , skin friction velocity in the same units as $U$ .
$V, V_p$		Functions used in the solution of equations (III-16), [VH, VHP].
$V_c$		Correction factor which accounts for influence of longitudinal wall curvature on the effective viscosity, [VHP].
$\overline{-v'h'}$		Reynolds heat flux.
$\overline{-v'u'}$		Reynolds stress.
$v_w$		Wall transpiration velocity in the same units as $U$ , [VW].
$x$		Streamwise coordinate; arbitrary dimensional units, [X].
$\Delta x$		$x_{i+1} - x_i$ , numerical integration step in the streamwise direction, [DX].
$y$		Coordinate normal to wall.
$y_s^*$		$s_w \sqrt{\tau_w/\rho_w}/\nu$ , wall roughness scaled on law of the wall coordinates [YPS].

$\alpha$	Angle of the tangent to the surface with respect to the axis of symmetry.
$\beta$	$\delta^*(dp/dx)/\tau_w$ , the Clauser equilibrium pressure gradient parameter, [B].
$\gamma =$	$\sqrt{\tau_w/\rho U^2}$ , ratio of skin friction velocity to freestream velocity, [GAM].
$\delta^* =$	$\int_0^\infty (\bar{\rho}_e \bar{U} - \bar{\rho} \bar{u})/(\bar{\rho}_e \bar{U}(r/r_w)) d\bar{y}$ , displacement thickness in the same units as $\bar{x}$ , [DT].
$\delta_k^* =$	$\int_0^\infty (\bar{U} - \bar{u})/\bar{U}(r/r_w) d\bar{y}$ , kinematic displacement thickness in the same units as $\bar{x}$ .
$\eta =$	$y/\delta^*$ , nondimensional coordinate normal to wall, [Y].
$\theta =$	$\int_0^\infty \bar{\rho} \bar{u} (\bar{U} - \bar{u})/(\bar{\rho}_e \bar{U}^2)(r/r_w) d\bar{y}$ , momentum thickness in the same units as $\bar{x}$ , [MT].
$\kappa =$	0.41, von Karman constant, [SK].
$\nu$	Molecular kinematic viscosity.
$\nu_e$	Effective kinematic viscosity (II-5a).
$\nu_{eg}$	Effective kinematic conductivity (II-5b).
$\nu_g$	Molecular kinematic conductivity (II-4b).
$\rho$	Density.
$\bar{\tau}$	Local shear stress (II-4a).
$T =$	$\nu_e/U\delta^*$ , nondimensional effective viscosity (II-17a), [VE].
$T^* =$	$R_{\delta^*} T$ , nondimensional effective viscosity in laminar starting flow, [VE].
$T_g =$	$\nu_{eg}/U\delta^*$ , nondimensional effective conductivity (II-17b), [VEG].
$\psi =$	$\int_0^\infty (\bar{\rho} \bar{u}/\bar{\rho}_e \bar{U})(\bar{h}_e^\circ - \bar{h}^\circ)/(\bar{h}_e^\circ - \bar{h}_r^\circ)(r/r_w) d\bar{y}$ , integral enthalpy thickness, [HF].
$\phi, \Phi$	Inner and outer effective viscosity functions shown in Figure 2.



- $X = \kappa y \sqrt{\tau/\rho} / \delta^* U$ , coordinate normal to wall in outer effective viscosity hypothesis, [CHI].
- $\chi = \kappa y \sqrt{\tau/\rho} / \nu$ , coordinate normal to wall in inner effective viscosity hypothesis.

### Superscripts and Subscripts

- $( )_a$  Evaluated at asymptotic matching point, [( )A].
- $( )_e$  Evaluated at edge of layer (except for  $v_e(\eta=\eta_e) \equiv v_{e\infty}$ ), also used to denote equilibrium  $f'$  and  $g'$  functions.
- $( )_w$  Evaluated at wall, [( )W].
- $( )_x$  Differentiation with respect to  $x$ .
- $( )_1$  Evaluated at initial  $x$  station.
- $( )_{\infty}$  Evaluated at the edge of the layer,  $\eta \rightarrow \infty$ , [( )E].
- $( )'$  Differentiation with respect to  $\eta = y/\delta^*$ , [( )P].
- $(\bar{\quad})$  Used with  $\bar{u}, \bar{v}$ , etc. denotes untransformed coordinates. Used with functions of  $x$  only, denotes average value,  $[( )_{i+1} + ( )_i]/2$ .
- $(\sim)$  Denotes quantity in similarity starting equations which have different interpretation in laminar and turbulent flows, see Section II, Initialization.
- $\$( )$  Denotes subroutine of program.

## I. INTRODUCTION

Studies of boundary layer flows have been made for two reasons; one is the practical need for boundary layer solutions in design problems; the other is the desire to achieve a better theoretical understanding of the mechanism of boundary layer flows. The calculation method described herein was designed to expedite both of these objectives. It makes recent advances in the state of the art available in the form of a convenient tool for those who are interested in ends rather than means. For those concerned with theoretical investigations of boundary layer flows, it overcomes the technical problems of solving the equations of motion and thereby emphasizes the physical assumptions necessary to circumvent our ignorance and inability to describe basic turbulent transport processes. A variety of assumptions can, therefore, be tested free from approximations related to the solution of the equations. Although a specific turbulent effective viscosity hypothesis is included in the program for practical calculations, it is wholly contained in a subroutine. The subroutine may easily be replaced by an alternative form.

The present report is an extension of Reference [1] to compressible flow. Also described are significant improvements and simplifications of the numerical method which apply to both incompressible and compressible versions of the program.

The compressible version of the program includes solution of the thermal energy equation and allows for necessary fluid property variations. Comparison of compressible flow data and heat transfer data may be found in Reference [2]. Somewhat more involved extensions of this program have also been used to investigate more complicated models which calculate mean turbulent energy fields and, at the Stanford Conference on Computation of Turbulent Boundary Layers [3], have been compared with calculations using the more simple effective viscosity hypothesis. This simple hypothesis performs remarkably well in predicting data and this has now been well documented in the literature [4,5,6]. Therefore, it is possible to concentrate on computational details in this report. Also, of course, the program can be operated entirely in a laminar mode where the problem is purely numerical.

Various versions of the program have now been in existence quite a number of years. However, it is one matter to have a program that works, but it is another matter to publish a program for general consumption to provide sufficient (though not exhaustive) documentation. Furthermore, considerable effort has now been expended to enable the program to handle flows of wide generality while avoiding numerical trauma.

Aside from the capability to compute planar or axisymmetric, laminar or turbulent variable property flows with arbitrary pressure gradients and heat transfer, provision has been made to calculate flows with longitudinal wall curvature, transpiration or aspiration and wall roughness. In these latter cases, predictability of data has not yet been documented in the literature; however, informal comparisons have been favorable. Internal means to effect transition from turbulent flow have not been provided; rather a transition factor (TURB), which varies from zero for laminar flow to unity for fully turbulent flow must be provided by the user as input. Undoubtedly, existing transition data could be incorporated in the program on a purely empirical basis, or, hopefully, a meaningful semi-empirical model of transition will be constructed in the future.

This manual is intended to be more than a catalog of the inputs and outputs. The boundary layer equations of motion are traced up to the point of being recast for computation in considerable detail. The alternative of reading in an initial profile or internally generating approximate laminar similarity (Falkner-Skan) or turbulent similarity (equilibrium) profiles is discussed. Then a step-by-step description of the function of each section of the program is given along with a flow chart and a list of notations. Finally, the practical problem of setting up the input parameters to calculate a specific flow is considered. Users who are not interested in the theoretical basis of the calculation method may skip directly to Section V, the description of inputs and outputs. Then if specific questions arise, reference can be made to earlier sections.

The basic numerical scheme can be described as an implicit, Crank-Nicholson method resulting at each station in an ordinary differential equation. The ordinary differential equation is solved using a Gaussian elimination method to solve the characteristic matrix. This method is

fast and stable and the split boundary conditions are simply satisfied in a single pass out and back through the layer.

A calculation method such as this must be regarded as flexible so that improvements can be readily incorporated as they become available. With this in mind, the guiding principle in the design of the Fortran coding was clarity of expression. Therefore algorithms were chosen which were primarily explicit, and easy to understand in order to conserve programming time, and only secondarily efficient in terms of calculation time. When calculation time becomes an important factor for a specific version of the program a competent systems programmer will be able to make the coding more expeditious possibly at the expense of clarity.

Two computer facilities were used at various times. One was the Princeton University Computer Center which is partially supported under National Science Foundation Grant NSF-6P579 and the other was made available by the Geophysical Fluid Dynamics Laboratory which is a division of NOAA.

## II. ANALYTICAL FUNDAMENTALS

### Equations of Motion

The equations governing the flow of a compressible, two-dimensional boundary layer illustrated in Figure 1, are\*

$$\frac{\partial r \bar{\rho} \bar{u}}{\partial \bar{x}} + \frac{\partial r \bar{\rho} \bar{v}}{\partial \bar{y}} = 0, \quad (\text{II-1})$$

$$\bar{\rho} \bar{u} \frac{\partial \bar{u}}{\partial \bar{x}} + \bar{\rho} \bar{v} \frac{\partial \bar{u}}{\partial \bar{y}} = \rho_e \bar{U} \frac{d\bar{U}}{d\bar{x}} + \frac{1}{r} \frac{\partial (r \bar{\tau})}{\partial \bar{y}}, \quad (\text{II-2})$$

$$\bar{\rho} \bar{u} \frac{\partial \bar{h}^\circ}{\partial \bar{x}} + \bar{\rho} \bar{v} \frac{\partial \bar{h}^\circ}{\partial \bar{y}} = \frac{1}{r} \frac{\partial}{\partial \bar{y}} [r(\bar{q} + \bar{u} \bar{\tau})] \quad (\text{II-3})$$

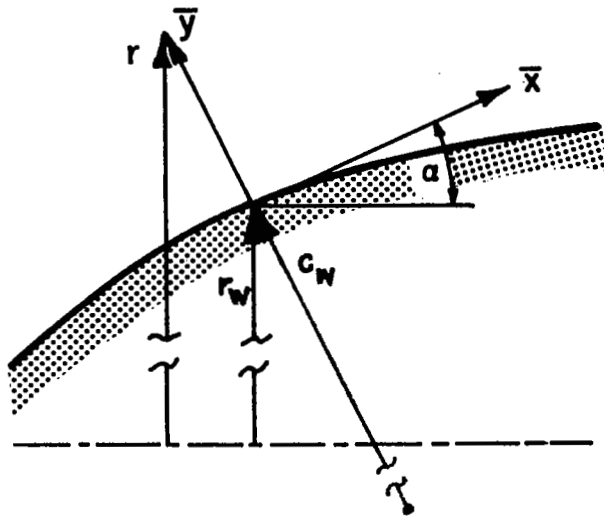
where  $r(\bar{x}, \bar{y}) = r_w(\bar{x}) + \bar{y} \cos \alpha(\bar{x})$  and  $\bar{h}^\circ = \bar{h} + \bar{u}^2/2$ . The equations apply to laminar or turbulent flow if the definition of  $\bar{\tau}$  and  $\bar{q}$  are taken to be

$$\bar{\tau}/\bar{\rho} = \bar{v} \frac{\partial \bar{u}}{\partial \bar{y}} - \overline{u'v'}, \quad (\text{II-4a})$$

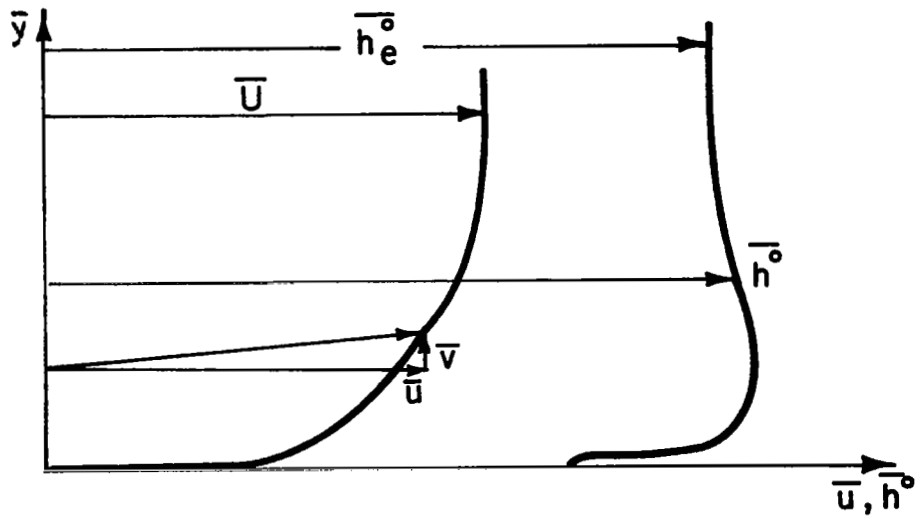
$$\bar{q}/\bar{\rho} = \bar{v} \frac{\partial \bar{h}}{\partial \bar{y}} - \overline{v'h'}, \quad (\text{II-4b})$$

---

\* The overbars are used to distinguish the untransformed variables from the transformed variables which are introduced later. However, the dependent variables should at all times be interpreted as time averaged quantities in tubulent flow.



a.) Coordinate System



b.) Description of Velocity and Total Enthalpy Profiles

Figure 1. Illustration of Notation

where  $-\overline{u'v'}$  is the kinematic Reynolds stress and  $-\overline{v'h'}$  is the kinematic Reynolds heat flux and  $\bar{h} = (\bar{p}/\bar{\rho})\gamma/(\gamma-1)$ . We next define an effective viscosity and an effective conductivity so that

$$\bar{\tau}/\rho = \nu_e (\partial\bar{u}/\partial\bar{y}) , \quad (\text{II-5a})$$

$$\bar{q}/\rho = \nu_{eg} (\partial\bar{h}/\partial\bar{y}) , \quad (\text{II-5b})$$

For laminar flow  $\bar{\nu}_e = \bar{\nu}$  and  $\bar{\nu}_{eg} = \bar{\nu}_g$ , the molecular kinematic viscosity and conductivity respectively.

The boundary conditions are

$$\bar{u}(\bar{x}, 0) = 0 , \quad (\text{II-6a})$$

$$\bar{v}(\bar{x}, 0) = \bar{v}_w(\bar{x}) \quad \text{or} \quad \bar{\rho}\bar{v}(\bar{x}, 0) = \bar{\rho}_w \bar{v}_w(\bar{x}) , \quad (\text{II-6b})$$

$$\lim_{\bar{y} \rightarrow \infty} \int_0^{\bar{y}} [\bar{\rho}_e \bar{U}(\bar{x}) - \bar{\rho}\bar{u}(\bar{x}, \bar{y}')] \left( \frac{r}{r_w} \right) d\bar{y}' \quad \text{is bounded,} \quad (\text{II-6c})$$

$$\bar{h}^\circ(\bar{x}, 0) = \bar{h}_w^\circ(\bar{x}) \quad \text{or} \quad \bar{q}(\bar{x}, 0) = \bar{q}_w(\bar{x}) , \quad (\text{II-6d})$$

$$\lim_{\bar{y} \rightarrow \infty} \int_0^{\bar{y}} \bar{\rho}\bar{u}[\bar{h}_e^\circ - \bar{h}^\circ(\bar{x}, \bar{y}')] \left( \frac{r}{r_w} \right) d\bar{y}' \quad \text{is bounded.} \quad (\text{II-6e})$$

For convenience it is useful to transform equations (II-1,2,3) so that they appear closer to their planar form. This can be accomplished with a variation of the Probstein-Elliott transformation, [8]. Thus,

$$x = \bar{x} \quad , \quad (II-7a)$$

$$y = \int_0^{\bar{y}} [r(\bar{x}, \bar{y}')/r_w] d\bar{y}' \quad , \quad (II-7b)$$

$$u(x, y) = \bar{u}(\bar{x}, \bar{y}) \quad , \quad (II-7c)$$

$$\rho(x, y) = \bar{\rho}(\bar{x}, \bar{y}) \quad , \quad (II-7d)$$

$$h^\circ(x, y) = \bar{h}^\circ(\bar{x}, \bar{y}) \quad . \quad (II-7e)$$

Using this transformation and the resulting relations

$$\frac{\partial}{\partial \bar{x}} = \frac{\partial}{\partial x} + \frac{\partial y}{\partial \bar{x}} \frac{\partial}{\partial y} \quad \text{and} \quad \frac{\partial}{\partial \bar{y}} = \frac{r}{r_w} \frac{\partial}{\partial y} \quad , \quad (II-8)$$

equations (II-1,2,3) become

$$\frac{1}{r_w} \frac{\partial r_w \rho u}{\partial x} + \frac{\partial \rho v}{\partial y} = 0 \quad , \quad (II-9)$$

$$\rho u \frac{\partial u}{\partial x} + \rho v \frac{\partial u}{\partial y} = \rho_e U \frac{dU}{dx} + \frac{\partial}{\partial y} \left[ \left( \frac{r}{r_w} \right) \bar{\tau} \right] \quad , \quad (II-10)$$

$$\rho u \frac{\partial h^\circ}{\partial x} + \rho v \frac{\partial h^\circ}{\partial y} = \frac{\partial}{\partial y} \left[ \frac{r}{r_w} (\bar{q} + u\bar{\tau}) \right] \quad , \quad (II-11)$$

where now  $\bar{\tau}/\rho = (r/r_w) v_e (\partial u/\partial y)$ ,  $\bar{q}/\rho = (r/r_w) v_{eg} (\partial h/\partial y)$ ,  
 $\rho v = (r/r_w) \bar{\rho} \bar{v} + y_{\bar{x}} \bar{\rho} \bar{u}$ , and  $r^2 = r_w^2(x) + 2y r_w(x) \cos \alpha(x)$ .

The form of the boundary conditions is unchanged.



$$u(x,0) = 0 , \quad (\text{II-12a})$$

$$v(x,0) = v_w(x) , \quad (\text{II-12b})$$

$$\lim_{y \rightarrow \infty} \int_0^y [U(x) - u(x,y')] dy' \text{ is bounded,} \quad (\text{II-12c})$$

$$h^\circ(x,0) = h_w^\circ(x) \quad \text{or} \quad \bar{q}(x,0) = \bar{q}_w(x) , \quad (\text{II-12d})$$

$$\lim_{y \rightarrow \infty} \int_0^y u[h_e^\circ - h^\circ(s,y')] dy' \text{ is bounded.} \quad (\text{II-12e})$$

For purposes of calculation it is convenient to define a new set of variables. The velocity and total enthalpy profiles are expressed in defect form

$$f'(x,\eta) = \frac{\rho_e U(x) - \rho u(x,y)}{\rho_e U(x)} , \quad (\text{II-13a})$$

$$g'(x,\eta) = \frac{h_e^\circ - h^\circ(x,y)}{h_e^\circ - h_r} , \quad (\text{II-13b})$$

$$d(x,\eta) = \frac{\rho_e(x)}{\rho(x,y)} , \quad (\text{II-13c})$$

$$\eta = \frac{y}{\delta^*(x)} . \quad (\text{II-13d})$$

The choice of (II-13a) is made because the calculation method is historically oriented toward turbulent flow in which case a defect formulation is convenient. Also some convenience results when considering outer boundary conditions. The coordinate,  $y$ , is normalized by  $\delta^*(x) = \int_0^\infty (\rho_e U - \rho u)/\rho_e U dy$ . The more conventional scaling for laminar flows would be

$\sqrt{U/\nu x}$ , but this is not meaningful in the turbulent case. Still no generality is lost since  $\delta^*$  will be proportional to  $\sqrt{U/\nu x}$  in the important Falkner-Skan laminar similarity flows. Finally, with an eye toward turbulent flows, the effective viscosity,  $\nu_e$  and  $\nu_{eg}$  are normalized on  $U\delta^*$  so that  $T = \nu_e/U\delta^*$  and  $T_g = \nu_{eg}/U\delta^*$  in turbulent flows  $T$  and  $T_g$  are prescribed functions of the local mean flow variables, whereas in laminar flows they are  $\nu/U\delta^*$  and  $\nu/U\delta^* P_r$  respectively.

When rewritten in terms of these variables, equations (II-9), (II-10), and (II-11) become

$$\begin{aligned}
 & - \left\{ (1 + C_a \eta) \frac{T}{d} [d(1-f')] \right\}' + \left\{ (Q + R) (\eta - f) - \frac{\rho_w^v w}{\rho_e U} - \delta^* f_x \right\} df'' \\
 & + \left\{ \left[ (Q + R) (\eta - f) - \frac{\rho_w^v w}{\rho_e U} - \delta^* f_x \right] d' - (Pd + \delta^* d_x) (2 - f') \right\} f' \\
 & - \left[ (Q + R) (\eta - f) - \frac{\rho_w^v w}{\rho_e U} - \delta^* f_x \right] d' + P(d-1) + \delta^* d_x \\
 & = (1 - f') \delta^* df'_x \tag{II-14}
 \end{aligned}$$

$$\begin{aligned}
 & \left[ (1 + C_a \eta) \frac{T_g}{d} \left\{ g'' - \frac{\frac{k-1}{2} M_e^2}{H \left( 1 + \frac{k-1}{2} M_e^2 \right)} \left( \frac{\nu_e}{\nu_{eg}} - 1 \right) [d^2(1-f')^2]' \right\}' \right] \\
 & + \left[ (Q + R) (\eta - f) - \delta^* f_x - \frac{\rho_w^v w}{\rho_e U} \right] g'' = (1 - f') \delta^* g'_x, \tag{II-15}
 \end{aligned}$$

$$d = \frac{2 \left[ 1 + \frac{k-1}{2} M_e^2 \right] (1 - Hg')}{1 + \sqrt{1 + 2(k-1) M_e^2 (1-f')} \left( 1 + \frac{k-1}{2} M_e^2 \right) (1 - Hg')} \tag{II-16}$$

where,  $P = \delta^* U_x / U$ ,  $Q = (\delta^* \rho_e U)_x / \rho_e U$ ,  $R = \delta^* r_w^x / r_w$ ,  $C_a = 2(\delta^* / r_w) \cos \alpha$ , and  $H = (h_e^\circ - h_r^\circ) / h_e^\circ$ . The form of the functions  $T$  and  $T_g$ , as given in Reference [2], is

$$T = \frac{\delta_k^*}{\delta^*} \left[ \frac{\phi(XR)}{\tilde{R}} + \Phi(X) - X \right], \quad (\text{II-17a})$$

and

$$T_g = \frac{\nu/\nu_\infty}{R_{\delta^* P_r}} + \frac{1}{P_{rt}} \left[ T - \frac{\nu/\nu_\infty}{R_{\delta^*}} \right], \quad (\text{II-17b})$$

where  $X = \kappa y \sqrt{\tau/\rho} / \delta_k^* U$ ,  $\tilde{R} = U \delta_k^* / \nu(\eta)$  and  $(\nu/\nu_\infty)$  are obtained from the Sutherland molecular viscosity relation,

$$\frac{\nu}{\nu_\infty} = \left( \frac{h}{h_e} \right)^{5/2} \frac{(h_e/C_p) + S_c}{(h/C_p) + S_c} \quad (S_c = 110^\circ \text{ Kelvin for air}). \quad (\text{II-18})$$

The functions  $\phi$  and  $\Phi$  are defined in Figure 2. Finally the boundary conditions are

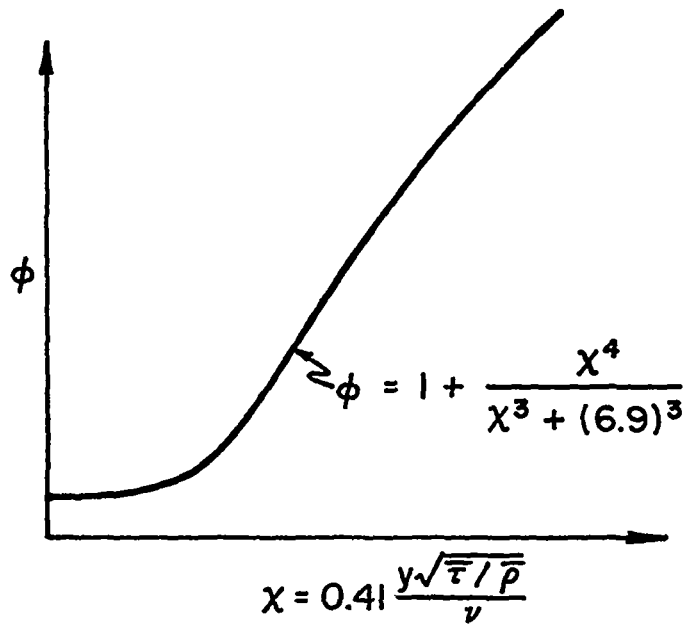
$$f(x,0) = 0, \quad (\text{II-19a})$$

$$f'(x,0) = 1, \quad (\text{II-19b})$$

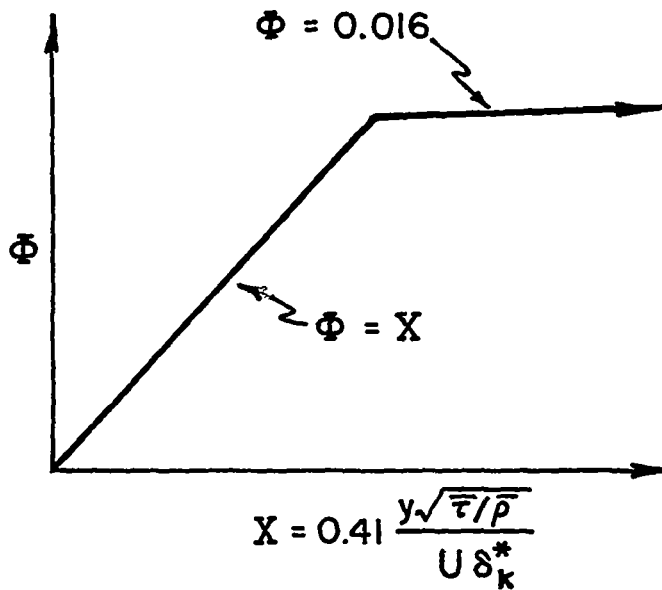
$$\lim_{\eta \rightarrow \infty} f(x,\eta) \rightarrow 1, \quad ** \quad (\text{II-19c})$$

---

\*\* The primary requirement is that  $f(\eta)$  be bounded as  $\eta \rightarrow \infty$ . However, so long as  $\eta = y/\delta^*$  the limit value is unity. On the other hand, throughout this text,  $\delta^*$  could be considered simply as an arbitrary scale length, where  $f(\infty)$  would assume the requisite value such that  $f(\infty)\delta^*$  is the real displacement thickness.



a.) The Inner Function,  $\phi = \phi(\chi)$



b.) The Outer Function,  $\Phi = \Phi(X)$

Figure 2. The Turbulent Effective Viscosity Hypothesis

$$g'(x,0) = \frac{h_e^\circ - h_w(x)}{h_e^\circ - h_r} \quad \text{or} \quad g''(x,0) = - \frac{\delta^* q_w(x)}{\rho_w v_w (h_e^\circ - h_r)}, \quad (\text{II-19d})$$

$$\lim_{\eta \rightarrow \infty} g(x,\eta) \quad \text{is bounded} \quad (\text{II-19e})$$

The complete set of equations described above is sufficient to calculate the development of a boundary layer. However, small inaccuracies in the numerical solution which are negligible after one step in  $x$ , are frequently cumulative. Greater accuracy can be achieved simply by correcting the integral parameters such as  $\delta^*$  and  $\theta$ , obtained from the numerical solution of equation (II-14), by referring to a numerically more accurate solution of the same equation. This form is obtained by first integrating equation (II-10) across the layer which yields the von Karman integral momentum equation.

$$\frac{d}{dx} (r_w \rho_e U^2 \theta) + r_w \delta^* \rho_e U \frac{dU}{dx} = r_w (\tau_w + \rho_w v_w U). \quad (\text{II-20})$$

Then, as suggested by Coles [9], equation (II-20) may be integrated with respect to  $x$  between two  $x$  stations  $x_{i-1}$  and  $x_i$ . The result is

$$\frac{\left[ \theta r_w \rho_e U^{2+H} \right]_i}{\left[ \theta r_w \rho_e U^{2+H} \right]_{i-1}} = \exp \left[ \int_{x_{i-1}}^{x_i} \left( \frac{\bar{C}_f}{2} + \frac{\rho_w v_w}{\rho_e U} \right) d \left( \frac{x}{\bar{\theta}} \right) \right] \quad (\text{II-21})$$

where  $\theta$ , the integral momentum thickness, is defined as

$$\theta = \int_0^\infty \frac{\rho u}{\rho_e U} \left( 1 - \frac{u}{U} \right) dy, \quad (\text{II-22})$$

where  $\bar{H}$ ,  $\bar{C}_f$ ,  $\bar{\theta}$  and  $(\overline{\rho_w v_w / \rho_e U})$  are average values in the interval  $(x_{i-1}, x_i)$ . Therefore, the left side, COF1, and right side, COF2, of (II-20) are first calculated and the calculated value  $\theta_i$  is corrected by multiplication with the ratio COF2/COF1. As an indication of the level of correction that has occurred, both COF1 and COF2 are printed out. Furthermore, if the finite difference solution were completely consistent, the left-hand side of equation (II-14) as evaluated from the results at any two stations  $i-1$  and  $i$ , and the right-hand side obtained from the average skin friction coefficient and transpiration rate in effect between  $i-1$  and  $i$  would be equal. The amount of imbalance is a check degree of accuracy of the finite difference solution.

A corresponding integral energy equation can be obtained by integrating equation (II-11) across the boundary layer and then with respect to  $x$  between  $x_{i-1}$  and  $x_i$ ,

$$\frac{\left[ r_w \rho_e U (h_e^\circ - h_r) \psi \right]_i}{\left[ r_w \rho_e U (h_e^\circ - h_r) \psi \right]_{i-1}} = \exp \left\{ \int_{x_{i-1}}^{x_i} \left( \bar{S}_{tr} + \left( \frac{\overline{\rho_w v_w}}{\rho_e U} \right) \left( \frac{h_e^\circ - h_w}{h_e^\circ - h_r} \right) d \left( \frac{x}{\psi} \right) \right) \right\}, \quad (II-23)$$

where  $\psi$ , the integral enthalpy thickness, is defined as,

$$\psi = \int_0^\infty \frac{\rho u}{\rho_e U} \left( \frac{h_e^\circ - h^\circ}{h_e^\circ - h_r} \right) dy \quad (II-24)$$

The left and right sides of equation (II-23), COG1 and COG2, respectively, are also printed as an indication of the accuracy of the numerical integration of equation (II-15).

## Initialization

In order to compute a solution of equations (II-14) and (II-15) it is necessary to prescribe the velocity and total enthalpy profiles at the first  $x$  station. Although one may read in these profiles as input data, often they are not readily known. What is likely to be known is the nature of the conditions under which the boundary layer developed in some region before the initial  $x$  station.

The difficulty here, which is not encountered in an incompressible flow, is that similarity solutions have not been found for the general case or compressible (laminar or turbulent) flows with heat transfer. Therefore, for the present purpose, a method of approximating these initial profiles has been provided which gives adequate results for more general cases and reduces to the exact solutions for incompressible flows. If more general similarity solutions become available they could be included at a later time. The two classes of approximate starting solutions which have been provided are generalizations of the Falkner-Skan family of laminar wedge flows including the flat plate and the stagnation point flow and the Clauser [10] equilibrium family for turbulent flows. Actually, most initial conditions of practical interest can be obtained accurately using these similarity solutions. The solutions for the whole class of laminar flows are correct since the flow in the immediate neighborhood of the forward stagnation point is both laminar and incompressible. Furthermore, both laminar and turbulent similarity solutions are exact at zero pressure gradient.

The calculation of these similar solutions requires relatively simple approximate specialization of equations (II-14), (II-15) and (II-16).

Approximate laminar similarity flow

To begin with, in the laminar, Falkner-Skan case, it is convenient to multiply the similarity version of equations (II-14) and (II-15) by  $R_{\delta^*}$ . Then setting  $f'_x = f_x = g'_x = 0$  the result is

$$\begin{aligned}
 & - \left\{ (1 + C_a \eta) \frac{T^*}{d} [d(1-f')] \right\}' + \left[ (Q^* + R^*) d(\eta-f) - d \frac{\rho_w^v w}{\rho_e U} R_{\delta^*} \right] f'' \\
 & + \left[ (Q^* + R^*) d'(\eta-f) - (P^* d + R_{\delta^*} \delta^* d_x) (2 - f') - \frac{\rho_w^v w}{\rho_e U} R_{\delta^*} d' \right] f' \\
 & + (Q^* + R^*) d' f + P^*(d-1) - (Q^* + R^*) \eta d' \\
 & + R_{\delta^*} \delta^* d_x + \frac{\rho_w^v w}{\rho_e U} R_{\delta^*} d' = 0 \tag{II-25}
 \end{aligned}$$

$$\begin{aligned}
 & \left[ (1 + C_a \eta) \frac{T^*}{d} \left\{ g'' - \frac{\frac{k-1}{2} M_e^2}{H \left( 1 + \frac{k-1}{2} M_e^2 \right)} \left( \frac{T^*}{T^* g} - 1 \right) [d^2(1-f')^2] \right\}' \right] \\
 & + \left[ (Q^* + R^*) (\eta - f) - \frac{\rho_w^v w}{\rho_e U} R_{\delta^*} \right] g'' = 0, \tag{II-26}
 \end{aligned}$$

where

$$R_{\delta^*} \delta^* d_x = \frac{P^*(k-1) M_e^2 \left( 1 + \frac{k-1}{2} M_e^2 \right) [1 - Hg' - d^2(1-f')^2]}{1 + (k-1) M_e^2 d(1-f')^2} \tag{II-27}$$



and  $P^* = \delta^{*2} U_x / \nu_\infty$ ,  $Q^* = R_{\delta^*} (\rho_e U \delta^*)_x / (\rho_e U)$ ,  $R^* = R_{\delta^*} r_{w_x} \delta^* / r_w$ ,

$T^* = TR_{\delta^*} = \nu(\eta) / \nu(\infty)$ ,  $T_g^* = T_g R_{\delta^*}$  and  $C_a$  is the quantity  $2(\delta^*/r_w) \cos \alpha$  evaluated at  $x_2^{**}$ .

The parameters  $P^*$ ,  $Q^*$  and  $R^*$  may be specified in two ways. One is by assuming the mainstream velocity distribution,  $U(x)$ , and displacement thickness  $\delta^*(x)$ , (see [11] page 143) to be of the form

$$\frac{U(x)}{U_L} = \left(\frac{x}{L}\right)^B \quad \text{and} \quad \frac{\delta^*(x)}{L} = C \left(\frac{x}{L}\right)^{\frac{1-B}{2}} \quad \text{respectively.} \quad (\text{II-28a,b})$$

A value of  $B = 0$  in the relations above corresponds to flat plate flow and  $B = 1$  corresponds to stagnation flow. Intermediate values of  $B$  represent wedge included angles of approximately  $2\pi B/(B+1)$  (radians). For cones  $B$  may also be related to the cone included angle; see, for example, Reference [12] page 428. The parameters needed to solve equation (II-25) and (II-26) can easily be shown to be

$$P^* = C^2 R_L^B, \quad (\text{II-29a})$$

$$Q^* = C^2 R_L \left[ B(1-M_e^2) + \frac{1}{2} (1-B) \right], \quad (\text{II-29b})$$

$$R^* = C^2 R_L L r_{w_x} / r_w, \quad (\text{II-29c})$$

where  $R_L = U_L L / \nu_\infty$  and  $C$  is determined in the course of solution so that  $f(\infty) = 1$ . Thus,  $R_L$ ,  $B$ , and  $L r_{w_x} / r_w$  specify the starting condition.

---

\*\*With the exception of the limit case of axisymmetric stagnation point flow, exact similarity solutions do not exist at the vertex of cones; where  $\delta^*/r_w$  is singular, the extent of the excluded region increases as the angle of the cone decreases. However, the procedure recommended here is probably sufficient to give good accuracy downstream of the vertex.

The other method of determining these parameters is to specify  $P^*$ ,  $R^*$ ,  $U\delta^*/\nu$  and  $(v_w/U) R_{\delta^*}$ . Then equation (II-25) may be integrated across the layer and the result solved for  $Q^*$ . In this case  $Q$  is evaluated iteratively in the course of obtaining a solution as described in Section III. The form of this integral is given below in conjunction with the turbulent case.

Approximate turbulent similarity flow

In the case of incompressible equilibrium turbulent flow, it is known that  $(U - u)/(\gamma U) \equiv f'_e (\gamma\gamma/\delta^*)$  is invariant with  $x$ , in which case (see Reference [4]),

$$\delta^* f'_{x} = \frac{\delta^* \gamma_x}{\gamma} \eta f' , \quad (\text{II-30a})$$

$$\delta^* f'_{x} = \frac{\delta^* \gamma_x}{\gamma} (\eta f'' + f') , \quad (\text{II-30b})$$

where  $\gamma = \sqrt{C_f/2}$ .

It is reasonable to make the same assumption for  $f'_e (\gamma\gamma/\delta^*) = (\rho_e U - \rho u)/\rho_e u_\tau$  and furthermore to assume  $g'_e$  to be of the form  $g'_e (\gamma\gamma/\delta^*) = [\rho_e u_\tau (h_e^\circ - h_e^\circ)]/q_w$  so that

$$\delta^* g'_{x} = \frac{\delta^* S_{tr_x}}{S_{tr}} g' + \frac{\delta^* \gamma_x}{\gamma} \eta g'' \quad (\text{II-31})$$

Finally, the exact expression for  $\delta^* d_x$  obtained from (II-16) is

$$\delta^* d_x = \frac{P(k-1) M_e^2 \left(1 + \frac{k-1}{2} M_e^2\right) [(1 - Hg') - d^2(1-f')^2]}{1 + (k-1) M_e^2 d(1-f')^2} + \frac{(k-1) M_e^2 d^2(1-f') \delta^* f'_{x} - \left(1 + \frac{k-1}{2} M_e^2\right) H \delta^* g'_{x}}{1 + (k-1) M_e^2 d(1-f')^2} . \quad (\text{II-32})$$

In constant property flow the factor  $\delta^* \gamma_x/\gamma$  can be obtained from the skin friction equation for equilibrium flow (see Reference [5]),

$$\frac{1}{\gamma} = \frac{1}{\kappa} \log_e \frac{\delta^* U}{v_\infty} + A(\beta) + B_s . \quad (\text{II-33})$$

Assuming this relation to be approximately valid for variable property flows yields

$$\frac{\gamma_x \delta^*}{\gamma} = - (\gamma/\kappa) (Q + C_\mu P), \quad (\text{II-34})$$

where

$$C_\mu = \left\{ 1.5 - \left[ 1 + \left( S_c C_p / h_e^\circ \right) \left( 1 + \frac{k-1}{2} M_e^2 \right) \right]^{-1} \right\} (k-1) M_e^2 . \quad (\text{II-35})$$

Furthermore, the Stanton number equation for constant property flow, which corresponds to (II-33), is of the form

$$\frac{\gamma}{S_{tr}} = \frac{1}{\kappa} \log_e \frac{\delta^* U}{v_\infty} + A_h(\beta) + B_h . \quad (\text{II-36})$$

Again taking this relation for variable property flow yields,

$$\frac{\delta^* S_{trx}}{S_{tr}} = - \frac{\gamma + S_{tr}/\gamma}{\kappa} (Q + C_\mu P) . \quad (\text{II-37})$$

Therefore, equations (II-14) and (II-15) may be rewritten in the form

$$\begin{aligned}
& - \left\{ (1 + C_a \eta) \frac{T}{d} [d(1-f')] \right\}' + \left\{ (Q + R) d(\eta-f) - \frac{\delta^* \gamma_x}{\gamma} \eta d - d \frac{\rho_w v_w}{\rho_e U} \right\} f'' \\
& + \left\{ (Q + R) d'(\eta-f) - (Pd + \delta^* d_x)(2-f') - (1-f')(d-\eta d') \frac{\delta^* \gamma_x}{\gamma} \frac{\rho_w v_w}{\rho_e U} d' \right\} f' \\
& + (Q + R) d'f + P(d-1) - (Q + R) \eta d' + \delta^* d_x + \frac{\rho_w v_w}{\rho_e U} d' = 0, \quad (II-38)
\end{aligned}$$

and

$$\begin{aligned}
& \left[ (1 + C_a \eta) \frac{T_g}{d} \left\{ g'' - \frac{\frac{k-1}{2} M_e^2}{H \left( 1 + \frac{k-1}{2} M_e^2 \right)} \left( \frac{T}{T_g} - 1 \right) [d^2(1-f')^2]' \right\} \right]' \\
& + \left\{ (Q + R)(\eta - f) - \frac{\delta^* \gamma_x}{\gamma} \eta - \frac{\rho_w v_w}{\rho_e U} \right\} g'' - (1-f') \frac{\delta^* S_{tr_x}}{S_{tr}} g' = 0. \quad (II-39)
\end{aligned}$$

It still remains to specify the parameters  $P$  and  $Q$ .  $P$  can be prescribed in two ways. One is to set  $\beta = (\delta^*/\tau_x) (dp/dx)$  from which

$$P = - (C_f/2)\beta. \quad (II-40)$$

This is quite satisfactory except for initial equilibrium boundary layers near separation. In that case, another approach is necessary since  $\beta \rightarrow \infty$  and  $C_f \rightarrow 0$ , making equation (II-40) impractical for numerical computation. However, as is shown in Reference [5],  $P$  is well behaved near separation and approaches the limit  $P = -0.00948$  in incompressible flow as  $\beta \rightarrow \infty$ . This limit is virtually independent of Reynolds number. Therefore, for large values of  $\beta$ , if  $P$  is fixed, the solution converges rapidly.

As in the laminar case,  $Q$  can be obtained from the integral of equation (II-38) across the layer. In both laminar and turbulent flow the resulting expression for  $Q$  is

$$Q = \frac{\frac{C_f}{2} + \int_0^{\infty} \left[ \begin{aligned} & [\tilde{R}d(\eta-f) + (\tilde{\gamma}/\kappa) C_{\mu} \tilde{P}nd - d(\rho_w v_w / \rho_e U)] f'' \\ & + [\tilde{R}d'(\eta-f) - (\tilde{P}d + \delta^* d_x)(2-f')] \\ & + (1-f')(d - \eta d')(\tilde{\gamma}/\kappa) C_{\mu} \tilde{P} - (\rho_w v_w / \rho_e U) d' ] f' \\ & + [\tilde{R}d'f + \tilde{P}(d-1) - \tilde{R}\eta d' + \delta^* d_x + (\rho_w v_w / \rho_e U) d' ] \end{aligned} \right] d\eta}{\int_0^{\infty} \left[ \begin{aligned} & [d(\eta-f) + (\tilde{\gamma}/\kappa)\eta d] f'' - (\eta-f) d' \\ & + [d'(\eta-f) + (1-f')(d - \eta d')(\tilde{\gamma}/\kappa)] f' \end{aligned} \right] d\eta} \quad \text{(II-41)}$$

where

$$\delta^* d_x = \frac{\tilde{P}(k-1) M_e^2 \left( 1 + \frac{k-1}{2} M_e^2 \right) [1 - Hg' - d^2(1-f')^2]}{1 + (k-1) M_e^2 d(1-f')^2} + \frac{(k-1) M_e^2 d^2(1-f') \frac{\delta^* \tilde{\gamma}_x}{\tilde{\gamma}} (f' + \eta f'')}{1 + (k-1) M_e^2 d(1-f')^2} - \frac{\left( 1 + \frac{k-1}{2} M_e^2 \right) H \left[ \frac{\delta^* \tilde{S}_{tr_x}}{\tilde{S}_{tr}} g' + \frac{\delta^* \tilde{\gamma}_x}{\tilde{\gamma}} g'' \eta \right]}{1 + (k-1) M_e^2 d(1-f')^2} \quad \text{(II-42)}$$

For laminar flow  $\tilde{P} = P^*$ ,  $\tilde{R} = R^*$  and  $\tilde{\gamma} = \delta^* \gamma_x / \gamma = \delta^* S_{tr_x} / S_{tr} = 0$ ,

whereas in turbulent flow  $\tilde{P} = P$ ,  $\tilde{R} = R$ ,  $\tilde{\gamma} = \sqrt{C_f/2}$  and  $\delta^* \gamma_x / \gamma$  and  $\delta^* S_{tr_x} / S_{tr}$  are given by equations (II-34) and (II-37) respectively.

### III. NUMERICAL METHOD

Equations (II-14) and (II-15) which describe the boundary layer flow, are nonlinear partial differential equations, parabolic in the flow direction. There are two phases of the procedure of obtaining a solution to these equations. The first phase is the conversion to ordinary differential equations using finite differences for the  $x$  derivatives. The second phase is the method or solution of the resulting ordinary differential equations.

#### Reduction to Ordinary Differential Equations

In the first phase, the  $x$  derivatives are represented by finite differences in the  $x$  direction according to an adaptation of the Crank-Nicholson [13] scheme. This method is of the implicit type. It is always stable and the error is of second order in the  $x$  step size.

The development of the difference equations is most clearly portrayed in three steps. The first step is to write equations (II-14) and (II-15) in terms of average functions at a point halfway between the  $x$  position of the known profiles,  $x_{i-1}$ , and that of the profiles to be calculated,  $x_i$ ,

$$\begin{aligned}
 & - \left\{ (1 + C_a \eta) \frac{\tau}{d} [d(1-f')] \right\}' + \left\{ (\bar{Q} + \bar{R})(\eta - \bar{f}) - (\bar{\rho}_w \bar{v}_w / \bar{\rho}_e \bar{U}) - \delta^* \bar{f}_x \right\} \bar{d} \bar{f}'' \\
 & + \left\{ [\bar{Q} + \bar{R})(\eta - \bar{f}) - (\bar{\rho}_w \bar{v}_w / \bar{\rho}_e \bar{U}) - \delta^* \bar{f}_x] \bar{d}' - (\bar{P} \bar{d} + \delta^* \bar{d}_x) (2 - \bar{f}') \right\} \bar{f}' \\
 & - [(\bar{Q} + \bar{R})(\eta - \bar{f}) - (\bar{\rho}_w \bar{v}_w / \bar{\rho}_e \bar{U}) - \delta^* \bar{f}_x] \bar{d}' + \bar{P}(\bar{d} - 1) + \delta^* \bar{d}_x \\
 & = (1 - \bar{f}') \delta^* \bar{d} \bar{f}'_x, \tag{III-1}
 \end{aligned}$$



$$\left[ (1 + C_a \eta) \frac{T_g}{d} \left\{ g'' - \frac{1/2(k-1)M_e}{H[1 + 1/2(k-1)M_e^2]} \left( \frac{T}{T_g} - 1 \right) [d^2(1-f')^2] \right\} \right]'$$

$$+ \left\{ (\bar{Q} + \bar{R})(\eta - \bar{f}') - (\bar{\rho}_w \bar{v}_w / \bar{\rho}_e \bar{U}) - \delta^* \bar{f}_x \right\} \bar{g}'' = (1 - \bar{f}') \delta^* \bar{g}_x' \quad (\text{III-2})$$

Then using the relations

$$\bar{f}' = 1/2(f'_i + f'_{i-1}), \text{ etc.} \quad (\text{III-3})$$

Equations (III-1) and (III-2) can be written in terms of functions at positions  $x_{i-1}$  and  $x_i$  as follows

$$\tau'_i = -\tau'_{i-1} + \bar{c}_1(f''_i + f''_{i-1}) + \bar{c}_2(f'_i + f'_{i-1}) + 2\bar{c}_3 - 2\bar{c}_4(f'_i - f'_{i-1}), \quad (\text{III-4})$$

$$g'_i = -g'_{i-1} + \bar{c}_7(g''_i + g''_{i-1}) - 2\bar{c}_8(g'_i - g'_{i-1}), \quad (\text{III-5})$$

where

$$\tau'_i = - \left\{ (1 + C_a \eta) T [f'' - (d'/d)(1-f')] \right\}'_i, \quad (\text{III-6a})$$

$$g'_i = - \left[ (1 + C_a \eta) \frac{T_g}{d} \left\{ g'' - \frac{(k-1)M_e^2}{H[1+1/2(k-1)M_e^2]} \left( \frac{T}{T_g} - 1 \right) d(1-f') [d'(1-f') - df''] \right\} \right]'_i, \quad (\text{III-6b})$$

$$\tau_{i-1} = c_{1_{i-1}} f''_{i-1} + c_{2_{i-1}} f'_{i-1} + c_{3_{i-1}} - c_{4_{i-1}} (f'_i - f'_{i-2}), \quad (\text{III-6c})$$

$$g'_{i-1} = c_{7_{i-1}} g''_{i-1} - c_{8_{i-1}} (g'_i - g'_{i-2}) , \quad (\text{III-6d})$$

and

$$c_0 = (Q + R)(\eta - f) - (\rho_w v_w / \rho_e U) - \delta^* f_x , \quad (\text{III-6e})$$

$$c_1 = c_0 d , \quad (\text{III-6f})$$

$$c_2 = c_0 d' - (Pd + \delta^* d_x)(2 - f') , \quad (\text{III-6g})$$

$$c_3 = -c_0 d' + P(d-1) + \delta^* d_x , \quad (\text{III-6h})$$

$$c_4 = d(1 - f')\delta^* / \Delta x , \quad (\text{III-6i})$$

$$c_7 = c_0 , \quad (\text{III-6j})$$

$$c_8 = (1 - f')\delta^* / \Delta x . \quad (\text{III-6k})$$

Finally the form in which these equations are solved is

$$[b_4(f'' + b_5)]'_i = b_3 + b_2 f''_i + b_1 f'_i , \quad (\text{III-7})$$

$$[b_4(g'' + b_5)]'_i = b_3 + b_2 g''_i + b_1 g'_i , \quad (\text{III-8})$$

where the coefficients for the  $f'$  equation are

$$b_1 = \bar{c}_2 - 2\bar{c}_4 + c_{4_{i-1}} , \quad (\text{III-9a})$$

$$b_2 = \bar{c}_1 , \quad (\text{III-9b})$$

$$b_3 = (\bar{c}_i - c_{i-1}) f''_{i-1} + (\bar{c}_2 + 2\bar{c}_4 - c_{2_{i-1}}) f'_{i-1} + 2\bar{c}_3 - c_3 - c_4 f'_{i-2}, \quad (\text{III-9c})$$

$$b_4 = - [(1 + C_a \eta) T]_i, \quad (\text{III-9d})$$

$$b_5 = - [(d'/d)(1-f')]_i, \quad (\text{III-9})$$

and for the  $g'$  equation

$$b_1 = \bar{c}_7, \quad (\text{III-10a})$$

$$b_2 = - 2\bar{c}_8 + c_{8_{i-1}}, \quad (\text{III-10b})$$

$$b_3 = (\bar{c}_7 - c_{7_{i-1}}) g''_{i-1} + 2\bar{c}_8 g'_{i-1} - c_{8_{i-1}} g'_{i-2}, \quad (\text{III-10c})$$

$$b_4 = - [(1 + C_a \eta) T_g/d]_i, \quad (\text{III-10d})$$

$$b_5 = - \left\{ \frac{(k-1) M_e^2}{H[1 + \frac{1}{2}(k-1) M_e^2]} \left( \frac{T}{T_g} - 1 \right) d(1-f') [d'(1-f') - df''] \right\}_i. \quad (\text{III-10e})$$

For the similarity starting flows, the corresponding coefficients of equation (III-7) are

$$b_1 = c_0 d' - (\tilde{P}d + \delta^* \tilde{d}_x) (2-f') - (1-f') (d - \eta d') (\delta^* \tilde{\gamma}_x / \tilde{\gamma}), \quad (\text{III-11a})$$

$$b_2 = [c_0 - \eta (\delta^* \tilde{\gamma}_x / \tilde{\gamma})] d, \quad (\text{III-11b})$$

$$b_3 = -c_0 d' + P(d-1) + \delta^* d_x, \quad (\text{III-11c})$$

$$b_4 = - (1 + C_a \eta) T, \quad (\text{III-11d})$$

$$b_5 = - (d'/d)(1-f'), \quad (\text{III-11e})$$

where  $c_0 = (\tilde{Q} + \tilde{R})(\eta-f) - (\rho_w v_w / \rho_e U)$ ,

$$b_1 = - (1-f')(\delta^* S_{tr_x} / S_{tr}), \quad (\text{III-12a})$$

$$b_2 = c_0 - \eta(\delta^* \gamma_x / \gamma), \quad (\text{III-12b})$$

$$b_3 = 0.0, \quad (\text{III-12c})$$

$$b_4 = - (1 + C_a \eta) T_g / d, \quad (\text{III-12d})$$

$$b_5 = - \frac{(k-1)M_e^2}{H_{1+1/2}^2 (k-1)M_e^2} \left( \frac{T}{T_g} - 1 \right) d(1-f') [d'(1-f') - df''], \quad (\text{III-12e})$$

The notation is as in equation (II-41) and  $\rho_w v_w / \rho_e U = R_{\delta^*}(\rho_w v_w / \rho_e U)$  in laminar flow and  $\rho_w v_w / \rho_e U = \rho_w v_w / \rho_e U$  in turbulent flow.

Because equations (III-1) and (III-2) are nonlinear, the solution is carried out iteratively. The coefficient  $b$  is evaluated using the result of the previous iteration. The resulting linear equation is then solved for  $f'$  and  $g'$ .  $\delta^*$  is adjusted so that  $f(\infty) = 1$  to some specified accuracy and the parameters  $P$ ,  $Q$ ,  $R$  and  $C_a$  are recalculated as are the effective viscosity functions,  $T$  and  $T_g$ . Then the cycle begins again. (To start the calculation at the new  $x$  station, the values of  $f'$  and  $g'$  from the previous  $x$  station and the parameters  $P$ ,  $Q$ ,  $R$  and  $C_a$  and the effective viscosity function are calculated based on an extrapolated value of  $\delta^*$ .)

## Solution of Ordinary Differential Equations

Equations of the form (III-7) are solved by applying a Gaussian elimination procedure to their characteristic matrices (see for example p. 200 of Reference [14]). This method is ideally suited for boundary layer equations because the problem of matching split boundary conditions is overcome so effortlessly.

In order to apply this method to equation (III-7),  $f'$ , for example, must be transformed according to the relation,

$$\hat{f}' = f' + \int_0^{\eta} b_5 d\eta . \quad (\text{III-13})$$

In terms of this variable equation (III-7) is written,

$$(b_4 \hat{f}'')' = b_2 \hat{f}' + b_1 \hat{f}' + b_3 - b_2 b_5 - b_1 \int_0^{\eta} b_5 d\eta . \quad (\text{III-14})$$

Through the use of relations such as

$$\hat{f}'_j = (\hat{f}'_{j+1} - \hat{f}'_{j-1}) / (\eta_{j+1} - \eta_{j-1}) , \quad (\text{III-15})$$

equation (III-14) can be expressed as a set of simultaneous equations

$$-a_{3j} \hat{f}'_{j+1} + a_{2j} \hat{f}'_j - a_{1j} \hat{f}'_{j-1} = a_{4j} , \quad (\text{III-16})$$

where the coefficients of the characteristic matrix are as follows,

$$a_{ij} = - \frac{\begin{pmatrix} b_{4j} & -b_{4j-1} \end{pmatrix}}{(\eta_{j+1} - \eta_{j-1})(\eta_j - \eta_{j-1})} - \frac{b_{2j}}{(\eta_{j+1} - \eta_{j-1})} , \quad (\text{III-17a})$$

$$a_{2j} = - \frac{1}{(\eta_{j+1} - \eta_{j-1})} \left[ \frac{b_{4j+1} + b_{4j}}{\eta_{j+1} - \eta_j} + \frac{b_{4j} + b_{4j-1}}{\eta_j - \eta_{j-1}} \right] - b_{1j} \quad , \quad (\text{III-17b})$$

$$a_{3j} = - \frac{(b_{4j+1} + b_{4j})}{(\eta_{j+1} - \eta_{j-1})(\eta_{j+1} - \eta_j)} + \frac{b_{2j}}{(\eta_{j+1} - \eta_{j-1})} \quad (\text{III-17c})$$

$$a_{4j} = b_{3j} - b_{2j} b_{5j} - b_1 \int_0^\eta b_5 d\eta \quad . \quad (\text{III-17d})$$

A solution for  $\hat{f}'_j$  can then be anticipated in the form

$$\hat{f}'_j = V_j \hat{f}'_{j+1} + V_{p_j} \quad . \quad (\text{III-18})$$

If (III-18) is substituted into (III-16),  $V_j$  and  $V_{p_j}$  are found to be

$$V_j = \frac{a_{3j}}{a_{2j} - a_{1j} V_{j-1}} \quad , \quad (\text{III-19a})$$

$$V_{p_j} = \frac{a_{4j} + a_{1j} V_{p_{j-1}}}{a_{2j} - a_{1j} V_{j-1}} \quad . \quad (\text{III-19b})$$

The first step of the procedure is to calculate the functions  $V$  and  $V_p$  across the layer beginning at the wall. The wall boundary conditions

are satisfied at this time using (III-13) and (III-18). For the momentum equation the boundary condition is

$$f'(x,0) = \hat{f}'(x,0) = 1.0 \quad (\text{III-20})$$

which can be achieved by setting

$$V_w = 0.0 , \quad (\text{III-21a})$$

$$V_{p_w} = 1.0 . \quad (\text{III-21a})$$

For the thermal energy equation the boundary condition with known wall enthalpy ratio is

$$g'(x,0) = \hat{g}'(x,0) = [h_e^\circ - h_w^\circ(x)] / (h_e^\circ - h_r^\circ) , \quad (\text{III-22})$$

and the corresponding values of  $V$  and  $V_p$  are

$$V_w = 0.0 , \quad (\text{III-23a})$$

$$V_{p_w} = [h_e^\circ - h_w^\circ(x)] / (h_e^\circ - h_r^\circ) . \quad (\text{III-23b})$$

The boundary condition for known Stanton number is

$$g''(x,0) = \hat{g}''(x,0) - b_5(0) = - S_{tr}(x) d(x,0) / T_g(x,0) , \quad (\text{III-24})$$

so that in this case  $V$  and  $V_p$  are given by

$$V_w = 1.0 , \quad (\text{III-25a})$$

$$V_{p_w} = - [-S_{tr}(x) d(x,0) / T_g(x,0) + b_5(0)] (\eta_2 - \eta_1) . \quad (\text{III-25b})$$

The complete  $f'$  or  $g'$  solution is then obtained from a combination of equations (III-13) and (III-18),

$$f'_j = V_j \left( f'_{j+1} + \int_0^{\eta_{j+1}} b_5 d\eta \right) - \int_0^j b_5 d\eta + V_{p_j}. \quad (\text{III-26})$$

The calculations begin with the freestream boundary conditions,  $f'(x, \infty) = g'(x, \infty) = 0.0$ , and proceed back from there to the wall.



## IV. COMPUTER PROGRAM

### Program Notation

Insofar as is possible the variable names in the subroutines are the same as those in the main program. It should be noted, however, that some variables which are subscripted in the main program are not subscripted in the subroutines although they are referred to by the same names.

A1...A4	Parameters in the Gaussian elimination method given in Section III, [a].
BB(K)	Dynamic storage in \$FILE.
B(J,K)	Coefficients in equations (III-7,8), $B(J,K) = b_K(\eta_J)$ .
BH =	$(h_e^\circ - h_r)/h_e^\circ$ , [H].
BK =	0.016, Clauser constant for outer portion of effective viscosity, [K].
B0...B5	Dynamic storage locations.
BS	Input for initial pressure gradient described in Section V, [B].
C	Constant in equation (II-28b) for laminar similarity solution, [C].
CA =	$2(\delta^*/r_w) \cos \alpha$ , [ $C_a$ ].
CA1 =	$(2/r_2) \cos \alpha$ .
CF =	$\tau_w / (\frac{1}{2} \rho U^2)$ , skin friction coefficient.
CHI =	$\kappa(y\sqrt{\tau_w/\rho\nu} + y_s^*)$ , coordinate normal to wall used in effective viscosity hypothesis, [ $\chi$ ].
CHI3 =	$\chi^3$ .
CMU	Parameter in equation (II-34), [ $C_\mu$ ].
CU =	$(\delta^*/c_w)(u/U) / [\partial(u/U)/\partial\eta]$ , longitudinal curvature parameter, [ $C_u$ ].

COAL  $\cos \alpha_1$ , cosine of angle of nose of axisymmetric body.

COF1 =  $(\theta r_w \rho_e U^{2+\bar{H}})_i / (\theta r_w \rho_e U^{2+\bar{H}})_{i-1}$ , left-hand side of equation (II-21).

COF2 =  $\exp \left\{ \int_{x_{i-1}}^{x_i} \left( \bar{C}_f / 2 + \overline{\rho_w v_w / \rho_e U} \right) d(x/\bar{\theta}) \right\}$ , right-hand side of equation (II-21).

COG1 =  $(\psi r_w \rho_e U)_i / (\psi r_w \rho_e U)_{i-1}$ , left-hand side of equation (II-23).

COG2 =  $\exp \left\{ \int_{x_{i-1}}^{x_i} \left[ \bar{S}_{tr} + \overline{(\rho_w v_w / \rho_e U) (h_e^o - h_w) / (h_e^o - h_r)} \right] d(x/\psi) \right\}$ , right-hand side of equation (II-23).

CW Longitudinal wall curvature in the same units as  $X$ ,  $[c_w]$ .

C0...C8 Coefficients given by equations (III-6),  $[c_0 \dots c_8]$ .

D =  $\rho_e / \rho$ , density ratio,  $[d]$ .

DB =  $(\rho_e / \rho)_{i-1}$ , density ratio at previous  $X$  station, also used in starting flow calculation to store  $\delta^* d_x$ .

DDX =  $\delta^* d_x$ .

DIVJ Number of divisions of input profile spacing in floating point form.

DOP Option number for input data, see Table 1b in Section V.

DT =  $\int_0^\infty (\bar{\rho}_e \bar{u} - \bar{\rho} \bar{u}) / \bar{\rho}_e \bar{u} (r/r_w) d\bar{y}$ , displacement thickness in the same units as  $X$ ,  $[\delta^*]$ .

DTM =  $1/2 (\delta_i^* + \delta_{i-1}^*)$ , intermediate value of  $\delta^*$ ,  $[\delta^*]$ .

DTS Value of displacement thickness before displacement thickness is altered to conform to integral momentum equation.

DTX =  $d\delta^*/dx$ .

DTXM =  $1/2 [(d\delta^*/dx)_i + (d\delta^*/dx)_{i-1}]$ , intermediate value of DTX,  $[\delta_x^*]$ .

DX =  $x_i - x_{i-1}$ ,  $x$  step size.

DY  $y$  step size in difference equations.

ET Value of  $f'$  at which calculation of profile stops,  $[f'_{\infty}]$ .

FJE =  $f(\infty)$ .

FLAG Device used to sense last X station input card.

FP =  $(\rho_e U - \rho u)/\rho_e U$ , velocity defect profile,  $[f']$ .

FPB Known  $f'$  profile at previous X station,  $[f'_b]$ .

FPPW Velocity defect gradient at wall,  $[f''_w]$ .

GAM =  $\sqrt{\tau_w}/\rho_e U^2$ , ratio of friction velocity to freestream velocity,  $[\gamma]$ .

GAMX =  $\gamma_X \delta^*/\gamma$ , shear stress gradient parameter in starting solution (II-34).

GBC The wall boundary condition on the energy equation, either  $g'_w = (h_e^{\circ} - h_w^{\circ})/(h_e^{\circ} - h_r^{\circ})$  or  $g''_w = -q_w \delta^*/\rho_w v_{ew} (h_e^{\circ} - h_r^{\circ})$ .

GP =  $(h_e^{\circ} - h^{\circ})/(h_e^{\circ} - h_r^{\circ})$ , total enthalpy defect profile,  $[g']$ .

GPW =  $(h^{\circ} - h_w^{\circ})/(h_e^{\circ} - h_r^{\circ})$ , value of  $g'$  at the wall,  $[g'_w]$ .

HB =  $(H_i + H_{i-1})/2$ , average shape factor.

HT =  $\int_0^{\infty} \bar{\rho} \bar{u} (h_e^{\circ} - \bar{h}^{\circ}) / [\bar{\rho}_e \bar{U} (h_e^{\circ} - h_r^{\circ})] (r/r_w) d\bar{y}$ , total enthalpy thickness in the same units as X,  $[\psi]$ .

I Index of functions of X for present calculation.

IB = I-1, index of functions of X for previous calculation.

IBC Index controlling mode of specifying wall boundary conditions on energy equation, see Table 1a in Section V.

ID Dimension of all functions of X.

IO Input parameter designated flow inside (IO = -1) or outside (IO = 1) of an axisymmetric body.

IOP Option number for initialization defined in Section V.

IS            Index of first X station for which  $U \neq 0$ .

IX            Total number of X station calculations read in ( $IX \leq ID$ ).

IXA          Total number of X station calculations actually performed.

IXF          Index of first X station calculation moving downstream.

J            Index of functions of  $\eta$ .

JD           Dimension of all functions of  $\eta$ .

JDIV        Number of subdivisions of input profile values.

JE           JEF or JEG, whichever is larger.

JEF          Index of last calculated  $f'$  profile value.

JEG          Index of last calculated  $g'$  profile value.

JEM        =     JE - 1.

JEP        =     JE + 1.

JF, JL      Indices of first and last points in each subdivision of the input profile.

JK           Index of the point at which the outer effective viscosity reaches a constant value (see Figure 2).

JLP        =     JL + 1.

JM         =     J - 1.

JP         =     J + 1.

JY           Index of largest  $\eta$  value read in ( $JY \leq JD$ ).

JYM        =     JY - 1.

KC           Number of iterations used to calculate  $T$  and  $\bar{\tau}$  from input profiles.

KMI         Maximum number of complete iterations allowed to calculate a profile.

LABEL       Storage for the label which appears on all output.

LOOP        Index of iterations to calculate profiles, whose maximum value is KMI.

LOOPF      Index of innerloop to calculate  $f'$  profile.

M	Freestream Mach number, $[M_e]$ .
ML	Freestream Mach number at $X = L$ , $[M_L]$ .
MOP	Option number controlling the mode of calculating the thermal energy, see Table 1a in Section V.
MR	Reference freestream Mach number.
MT	= $\int_{\rho}^{\infty} \rho \bar{u} (\bar{U} - \bar{u}) / \rho_e \bar{U}^2 (r/r_w) d\bar{y}$ , momentum thickness in the same units as $X$ , $[\theta]$ .
NU	= $Lg_w / [\rho_e \nu_{g\infty} (h_e^{\circ} - h_w)]$ , the Nussett number.
OI	Floating point value of IO.
P	= $\delta^* U_x / U$ , parameter in equation (II-14), $[P]$ .
PB	Value of $P$ at previous $X$ station.
PM	= $1/2(P + PB)$ , intermediate value of $P$ , $[\bar{P}]$ .
PR	Molecular Prandtl number, $[P_r]$ .
PRT	Turbulent Prandtl number, $[P_{rt}]$ .
Q	= $(\rho_e U \delta^*)_x / \rho_e U$ , parameter in equation (II-14), $[Q]$ .
QM	= $1/2(Q + QB)$ , intermediate value of $Q$ , $[\bar{Q}]$ .
QRM	= $\bar{Q} + \bar{R}$ .
R	= $r_{wx} \delta^* / r_w$ , parameter in equation (II-14).
RB	Value of $R$ at previous $X$ station.
RDF	= $R_{\delta^*}$ , = 0 (laminar starting flow); = 1 (turbulent starting flow).
RDT	= $U \delta^* / \nu_{\infty}$ , Reynolds number based on displacement thickness.
RL	= $UL / \nu_{\infty}$ , Reynolds number used in laminar similarity solution.
RM	= $1/2(R + RB)$ , intermediate value of $R$ , $[\bar{R}]$ .
RW	Radius of surface body in the same units as $X$ , $[r_w]$ .

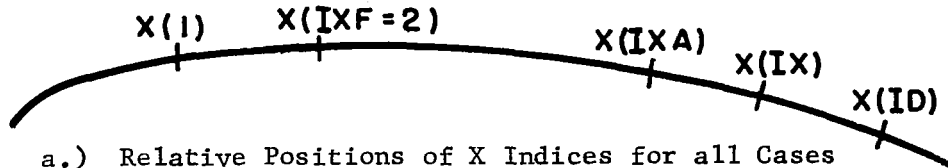
RX =  $r_{w_x}/r$ .  
 SF =  $\delta^*/\theta$ .  
 SHR =  $C_p/C_v$ , specific heat ratio, [k].  
 SIG3 =  $(6.9)^3$ , empirical constant in the effective viscosity for the wall layer.  
 SK = 0.41, von Karman constant in empirical effective viscosity.  
 ST =  $q_w/[\rho_e U(h_e^\circ - h_w)]$ , Stanton number based on freestream to wall enthalpy difference, [ $S_t$ ].  
 STC Constant  $S_c$  in degrees Kelvin used in the Sutherland viscosity formula, (II-18).  
 STR =  $q_w/\rho_e U(h_e^\circ - h_r)$ , Stanton number based on freestream to reference enthalpy difference, [ $S_{tr}$ ].  
 STRX =  $S_{tr_x} \delta^*/S_{tr}$ , Stanton number gradient parameter in starting solution (II-37).  
 SW Nikuradse [15] sand grain roughness scale in the same units as  $X$ , [ $s_w$ ].  
 TAU =  $\bar{\tau}/\rho_e U^2$ , nondimensional local shear stress.  
 TF =  $1 + \frac{1}{2}(k - 1)M_e^2$ .  
 TFR =  $1 + \frac{1}{2}(k - 1)M_r^2$ .  
 TO Freestream total temperature in degrees Kelvin.  
 TURB Input parameter which indicates what proportion ( $0.0 \leq \text{TURB} \leq 1.0$ ) of effective viscosity is laminar and what part turbulent, [T].  
 U = Freestream velocity at each  $X$  station; arbitrary dimensional units, [U].  
 UX =  $U_x/U$ .  
 U+ =  $u/u_\tau$ , "law of the wall" velocity.

VE	Nondimensional effective viscosity (II-17a), [T].
VEG	Nondimensional effective conductivity (II-17b), [T <sub>g</sub> ].
VH, VHP, VHPP	Dynamic storage
VP =	$\rho_w v_w / \rho_e U$ , in turbulent flow and $(\rho_w v_w / \rho_e U) R_{\delta^*}$ , in laminar flow (see Table 1b).
VR	Value of T in outer part of turbulent layer.
VW	Transpiration velocity in the same units as U which may be density weighted as explained in Table 1b.
X	Input values of x at which calculations are to be performed; arbitrary dimensional units, [x].
XT	Convergence criteria specifying maximum allowable variation between results of consecutive iterations.
Y =	$y/\delta^*$ independent variable normal to the wall, [ $\eta$ ].
YPS	Empirical effective roughness scale in law of the wall form, [ $y_s^*$ ].
YY =	$\bar{y}/\delta^*$ , in untransformed coordinates, see equation (II-7b).
YY+ =	$yu_\tau/\nu$ , independent variable in "law of the wall" region.
ZERO	Very small constant.

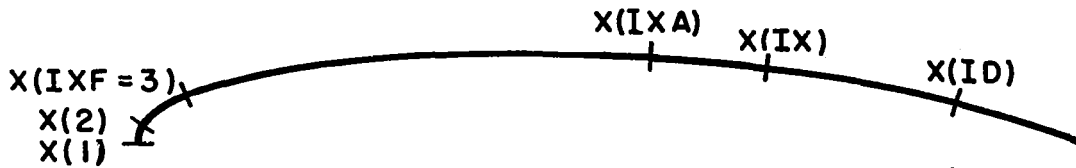
#### Naming Conventions

( )B	Variable at previous X station, [( ) <sub>b</sub> ].
( )E	Function of $\eta$ evaluated at freestream.
( )P	Derivative with respect to $\eta$ , [( )'].
( )W	Function of $\eta$ evaluated at wall, [( ) <sub>w</sub> ].
( )1,2	Function of $\eta$ evaluated at $\eta_{j+1}$ .
\$( )	Denotes subroutine of the program.

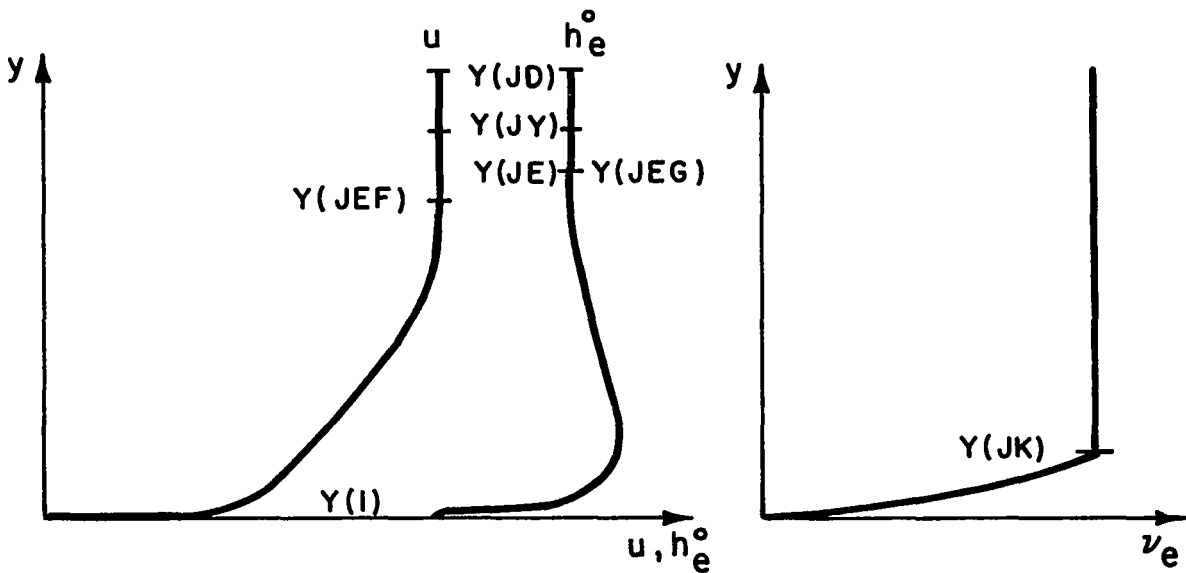
The relative locations of the X and Y indices are illustrated in Figure 3.



a.) Relative Positions of X Indices for all Cases Except Option 4 of Section V.



b.) Relative Positions of X Indices for Option 4 of Section V.



c.) Relative Positions of Y Indices for Turbulent Flow. In Laminar Flow, Since  $v_e = v$ , JK is Arbitrarily Set Equal to JE.

Figure 3. Illustrations of Meaning of Indices Used in X and Y Notation.



## Main Program

The program divides naturally into two parts, as is reflected in the flow chart shown in Figure 4. The first part is concerned with the preparation of an appropriate  $f'(\eta)$  and  $g'(\eta)$  profiles and associated parameters for the initial  $x$  station. The second half carries the computation forward to successive  $x$  stations. Many of the computational patterns are similar in the two parts and it might seem that the two could be efficiently combined. However, the differences are fundamental enough so that the cause of clarity is best served by keeping them separate.

The first few instructions read in all of the input data required. The appropriate formats for the data and the requirements on the inputs are treated in Section V. Next, the related profiles  $f(\eta)$ ,  $f''(\eta)$ ,  $g(\eta)$ ,  $g''(\eta)$  and  $\tau(\eta)$  are calculated from the input  $f'(\eta)$  and  $g'(\eta)$ . Then all of the input information and related profiles are printed out for reference. If an approximate similarity solution is to be used to start the boundary layer, the input profiles are merely a rough guess. In this case, the program recalculates the initial profiles in the iterative loop which follows. If the input profiles are to be used as they are this recalculation is not performed. Finally, in either case, several other initial parameters are calculated and the initial profiles and parameters are printed out in their final form. This is the end of the initialization portion of the program.

The forward motion part of the program consists of a loop which cycles for each  $x$  station calculation. The loop begins by moving the known profile into storage for the profile at the  $x$  station before the one to be calculated. Then the input boundary conditions are printed out for reference. This is followed by the iterative loop to calculate a new set of profiles at the  $x$  station. Within this loop, there is an inner loop to iterate for the  $f'$  profile. When these calculations have converged integral parameters for that position are calculated and the integral test for accuracy is

printed out. This process continues until profiles have been calculated at all x stations. Finally, for convenience, a summary of the parameters of the flow is printed out.

A listing of the program follows. The numbers in parentheses along the right-hand margin of the listing refer to equation numbers in Sections II and III.

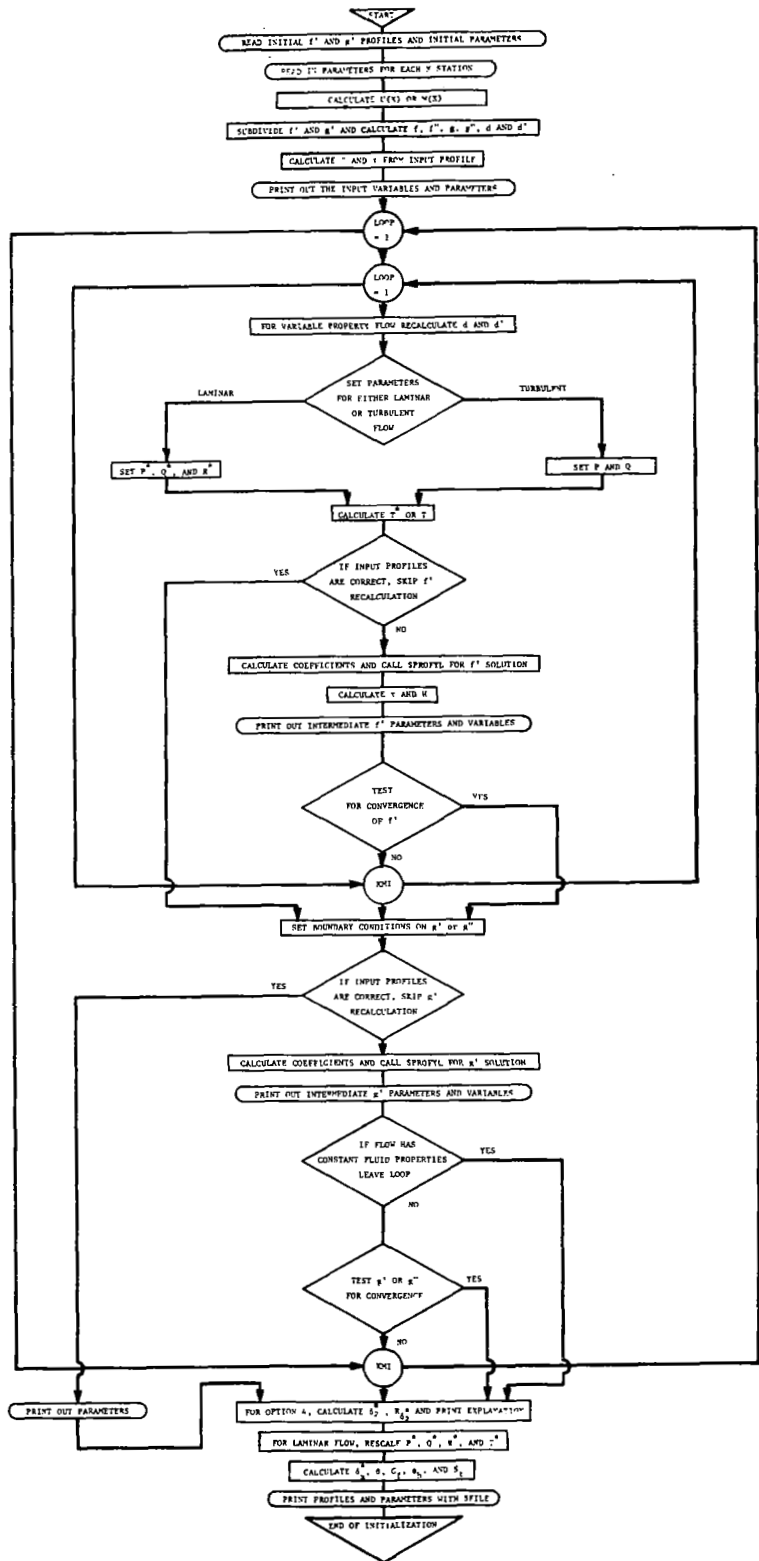


Figure 4a. Flow Chart for the Initialization Section of the Main Program.

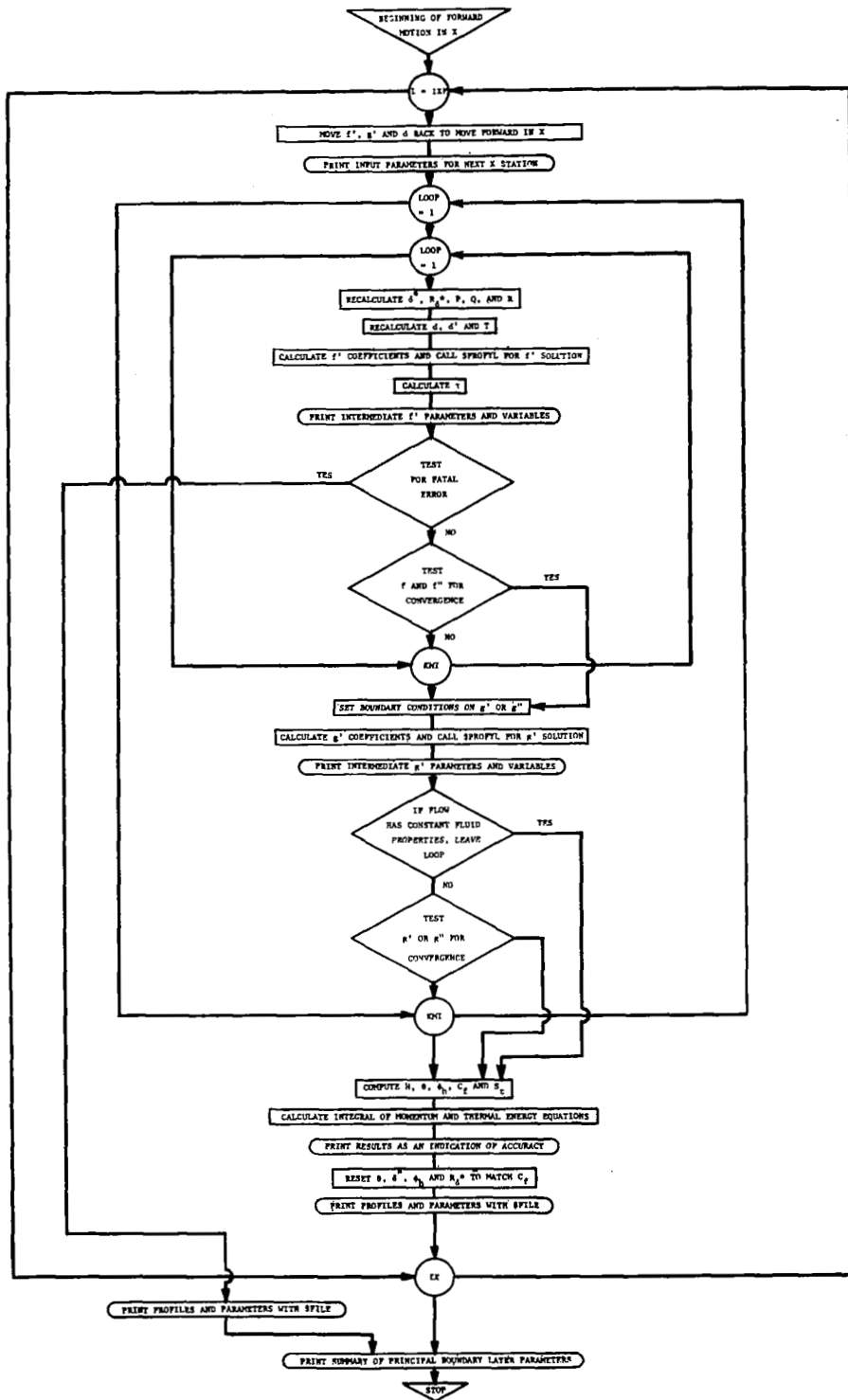


Figure 4b. Flow Chart for the Forward Motion Section of the Main Program.

CCCCCCCCCCCC

THIS COMPUTER PROGRAM PERFORMS A NUMERICAL INTEGRATION OF THE EQUATIONS OF MOTION FOR A COMPRESSIBLE TWO-DIMENSIONAL BOUNDARY LAYER. BOUNDARY LAYER CALCULATIONS MAY BE CARRIED OUT FOR BOTH LAMINAR AND TURBULENT FLOW FOR ARBITRARY REYNOLDS NUMBER AND FREESTREAM MACH NUMBER DISTRIBUTION, ON PLANAR OR AXISYMMETRIC BODIES WITH WALL HEATING OR COOLING, WALL SUCTION OR BLOWING AND WITH A ROUGH OR A SMOOTH WALL.

THIS PROGRAM WAS DEVELOPED UNDER GRANT NGR 31-001-074 FROM NASA-LEWIS.

H. JAMES HERRING AND GEORGE L. MELICR  
PRINCETON UNIVERSITY

DIMENSION Y(300), YY(300), B(300,5), LABEL(18)  
DIMENSION VE(300), VEG(300), TAU(300)  
DIMENSION F(300), FP(300), FPP(300), FB(300), FPB(300), FPPB(300)  
DIMENSION GP(300), GPP(300), GPB(300), GPPB(300)  
DIMENSION D(300), DP(300), DB(300), DPP(300)  
DIMENSION FEE(300), FPBB(300), GPBB(300), DBB(300)  
DIMENSION VH(300), VHP(300), VHPP(300)  
DIMENSION X(60), U(60), M(60), TURB(60), GBC(60), RW(60), VW(60)  
DIMENSION SW(60), CW(60), DT(60), MT(60), SF(60), HT(60), RDT(60)  
DIMENSION CF(60), ST(60), STR(60), GPW(60), TF(60), DTK(60)  
REAL M, ML, MR, MT, NU  
INTEGER DCP  
DATA ID, JD, KMI/ 60, 300, 10/  
DATA YY, F, FP, FPP/ 300\*0.0, 300\*0.0, 300\*0.0, 300\*0.0/  
DATA GP, GPP/ 300\*0.0, 300\*0.0/  
DATA D, DP, DB, TAU/ 300\*1.0, 300\*0.0, 300\*0.0, 300\*0.001/  
DATA VH, VHP, VHPP/ 300\*0.0, 300\*0.0, 300\*0.0/  
DATA B/ 1500\*0.0/  
DATA DT, MT, SF, HT, RDT/ 60\*0.0, 60\*0.0, 60\*0.0, 60\*0.0, 60\*0.0/  
DATA CF, ST, STR, GPW, TF/ 60\*0.0, 60\*0.0, 60\*0.0, 60\*0.0, 60\*0.0/  
DATA ET, XT/ 1.0E-08, 0.005/  
DATA SHR, STC, PR, PRT/ 1.4, 110.0, 0.78, 1.0/  
DATA SK, BK/ 0.41, 0.016/  
DATA ZERO/ 1.0E-16/  
WRITE (6,99)

100 CONTINUE

C \*\*\*\* READ IN INITIAL FP AND GP PROFILES AND INITIAL PARAMETERS \*\*\*\*

READ (5,1) (LABEL(K), K=1,18)  
READ (5,2) JIIV  
READ (5,2) JY  
JY=(JY-1)\*JDIV+1  
READ (5,3) (YY(J), J=1, JY, JDIV)  
READ (5,2) JEF  
JEF=(JEF-1)\*JDIV+1  
READ (5,3) (FP(J), J=1, JEF, JDIV)  
READ (5,2) JEG  
JEG=(JEG-1)\*JDIV+1  
READ (5,3) (GP(J), J=1, JEG, JDIV)  
READ (5,2) ICP, MOP, DCE, IO  
READ (5,3) MR, DT(1), FDT(1), BS, TC, BH

C \*\*\*\* READ IN PARAMETERS FOR EACH X STATION \*\*\*\*

DO 101 I=1, ID  
READ (5,4) X(I), U(I), TURB(I), GBC(I), RW(I), VW(I), SW(I), CW(I)  
IF (X(I).LT.-1000.0) GO TO 102  
IX=I

101 CONTINUE

READ (5,4) FLAG

102 CONTINUE

1 FORMAT (18A4)  
2 FORMAT (16I5)  
3 FORMAT (6F10.5)  
4 FORMAT (8F10.5)

RL=RDT(1)

ML=MR

TFR=1.+(SHR-1.)/2.\*MR\*MR

C \*\*\*\* CALCULATE U(X) OR M(X) \*\*\*\*

IS=1

IF (ICP.EQ.4) IS=2

```

IF (MR.LT.ZERO.OR.DOP.GT.C) GO TO 105
DO 104 I=1, IX
M(I)=U(I)
TF(I)=1.+(SHR-1.)/2.*M(I)*M(I)
U(I)=M(I)/MR*SCRT(TFR/IF(I))
104 CONTINUE
GO TO 107
105 CONTINUE
DO 106 I=1, IX
M(I)=U(I)/U(IS)*MR
1 /SQRT(1.+(SHR-1.)/2.*MR*MR*(1.-U(I)*U(I)/U(IS)/U(IS)))
TF(I)=1.+(SHR-1.)/2.*M(I)*M(I)
106 CONTINUE
107 CONTINUE
C **** SUBDIVIDE FP AND GP AND CALCULATE F, FPP, G, GPP, D AND DP ****
DIVJ=JDIV
DO 108 J=2, JY
JF=(J-1)/JDIV*JDIV+1
JL=(J+JDIV-2)/JDIV*JDIV+1
YY(J)=YY(JF)+(YY(JL)-YY(JF))/DIVJ*FLOAT(J-JF)
FP(J)=FP(JF)+(FP(JL)-FP(JF))/DIVJ*FLCAT(J-JF)
GP(J)=GP(JF)+(GP(JL)-GP(JF))/DIVJ*FLOAT(J-JF)
108 CCNTINUE
JE=MAXG(JFF,JEG)
CMTF=1.0
CMTG=1.0
P=BS
OI=IO
R=C.C
CA=1.0
SC=1.0
I=1
IF (IC.NE.C) SC=C.5
GO TO (113,114,114,112,113,114,114), IOP
112 CONTINUE
I=2
C=SQRT(2./(BS+1.)/RL)
P=C*C*RL*BS
RDF=C*RL
RDT(2)=RDF
COAL=SQRT(1.-((RW(2)-RW(1))/(X(2)-X(1)))**2)
IF (ABS(RW(2)/(X(2)-X(1))).LT.1.E-8) GO TO 115
R=RL*C*C*(RW(3)-RW(1))/(X(3)-X(1))*X(2)-X(1)/(RW(3)+RW(1))
CA=2.*OI*COAL*C*(X(2)-X(1))/PW(2)
GO TO 115
113 CCNTINUE
RDF=RDT(I)
IF (ABS(RW(1)/DT(1)).LT.C.1) GO TO 115
R=(RW(2)-RW(1))/(X(2)-X(1))*DT(1)/RW(1)*RDT(1)
CA=2.*OI*DT(1)/RW(1)*SQRT(1.-((RW(2)-RW(1))/(X(2)-X(1)))**2)
GO TO 115
114 CCNTINUE
RDF=1.C
IF (ABS(RW(1)/DT(1)).LT.0.1) GO TO 115
R=(RW(2)-RW(1))/(X(2)-X(1))*DT(1)/RW(1)
CA=2.*OI*DT(1)/RW(1)*SQRT(1.-R/DT(1)*RW(1)*R/DT(1)*RW(1))
115 CONTINUE
DO 120 J=1, JD
Y(J)=YY(J)*(1.+YY(J)*CA/4.)
120 CONTINUE
IF (IABS(DOP).NE.1.CR.MCP.LT.C) GO TO 123
DO 122 J=1, JE
FV=1.-FP(J)
FP(J)=1.-FV/(TF(I)*(1.-GP(J)*BH)-(TF(I)-1.)*FV*FV)
122 CONTINUE
123 CONTINUE
CALL INTEG (JE, JD, Y, FP, F)
DO 125 J=1, JY
JP=J+1-J/JY
JM=J-1+1/J
DY=Y(JP)-Y(JM)
FPP(J)=(FP(JP)-FP(JM))/DY
GPP(J)=(GP(JP)-GP(JM))/DY

```

```

125 CONTINUE
  IF (MOP.LT.0) GO TO 127
  B1=TF(I)-1.
  DO 126 J=1, JY
  FV=1.-FP(J)
  D(J)=2.*TF(I)*(1.-BH*GP(J))/(1.+SQRT(1.+4.*B1*FV*FV*TF(I)
  1 * (1.-BH*GP(J))))
  DP(J)=(2.*B1*D(J)*D(J)*FV*FPP(J)-TF(I)*BH*GPP(J))
  1 / (1.+2.*B1*D(J)*FV*FV) (II-16)
126 CONTINUE
  DP(JY)=0.0
127 CONTINUE
  DO 128 J=1, JE
  FV=1.-FP(J)
  VH(J)=FV*(1.-D(J)*FV)
128 CONTINUE
  CALL INTEG (JE, JD, Y, VH, 0.0, VH)
  SF(1)=1./VH(JE)
  MT(1)=DT(1)/SF(1)
  Q=0.0
  CMU=(1.5-1./(1.+STC/T0*IFR))*(SHR-1.)*MR*MR (II-35)
  GAM=0.0
  GAMX=0.0
  STRX=0.0
C **** CALCULATE VE AND TAU FROM INPUT PROFILE ****
  KC=5
  IF (TURB(I).LT.1.0) KC=1
  DO 132 K=1, KC
  CALL VIS (JE, JY, JD, YY, FP, FPP, GP, GPP, D, DP, TAU, VH, VHP,
  1 TURB(I), SW(I), CW(I), SHR, BH, STC, T0, TF(I), RDT(I), DT(I),
  2 P(JY), PR, PRT, JK, VE, VEG)
  DO 131 J=1, JY
  TAU(J)=VE(J)*(DF(J)/D(J)*(1.-FP(J))-FPP(J))*SQRT(1.+CA*Y(J))
131 CONTINUE
132 CONTINUE
  IF (TURB(I).GT.0.999) CF(I)=2.*TAU(I)
C **** PRINT OUT THE INPUT VARIABLES AND PARAMETERS ****
  CALL FILE (LABEL, I, YY, F, FP, FPP, GP, GPP, D, DP,
  1 VH, VHP, VHPP, TAU, VE, VEG, SHR, BH, PR, PRT,
  2 X, U, M, TURB, RW, VW, SW, CW,
  3 RDT, DT, MT, HT, SF, CF, ST, STR, ID, JE, JY, JD, JDIV)
  WRITE (6,51) (LABEL(K), K=1,18)
  WRITE (6,52) JDIV
  WRITE (6,53) SHR, PR, PRT
  WRITE (6,54) FT, XT
  WRITE (6,55) ICP, MOP, DOP, IO
  WRITE (6,56) M(1), DT(1), RDT(1), BS, T0, BH
  WRITE (6,6) X(1), U(1), M(1), TURB(1), GBC(1), RW(1), VW(1),
  1 SW(1), CW(1)
  IF (IOP.EQ.4)
  1 WRITE (6,6) X(2), U(2), M(2), TURB(2), GBC(2), RW(2), VW(2),
  1 SW(2), CW(2)
51 FORMAT (1H, 9X, 2: HINEUT VARIABLES FOR , 18A4)
52 FORMAT (1X, 6HJDIV =, I2)
53 FORMAT (1X, 5HSHR =, F5.2, 2X, 4HPP =, F6.2, 2X, 5HPRT =, F6.2)
54 FORMAT (1X, 4HFT =, 1PE9.2, 2X, 4HXT =, 1PE9.2)
55 FORMAT (1X, 5HIOP =, I2, 2X, 5HMOP =, I2, 2X, 5HDOP =, I2, 2X,
  1 4HIO =, I2)
56 FORMAT (1X, 3HM =, F6.2, 2X, 4HDT =, 1PE9.2, 2X, 5HRDT =, E9.2,
  1 2X, 3HB =, E9.2, 2X, 4HT =, E9.2, 2X, 4HBH =, E9.2)
6) FORMAT (1H, 9X, 3HX =, 1PE9.2, 1X,
  1 3HU =, F9.2, 1X, 3HM =, E9.2, 1X, 6HTURB =, JPF5.2, 1X,
  2 5HGBC =, 1PE9.2, 1X, 4HRW =, F9.2, 1X, 4HVW =, E9.2,
  3 1X, 4HSW =, E9.2, 1X, 4HCW =, E9.2)
98 FORMAT (1H)
99 FORMAT (1H)
  WRITE (6,7)
  WRITE (6,71)
70 FORMAT (1H) 4X
  1 48HVALUES OF IMPORTANT VARIABLES FOR EACH ITERATION)
71 FORMAT (1H, 1HF, 2X, 2HJK, 1X, 3HJEP, 5X, 3HFJE, 6X, 4HFPPW,
  1 6X, 2HSP, 9X, 1HP, 9X, 1HO, 9X, 1HR, 1X, 1HG, 5X,
  2 3HJEG, 5X, 3HGPW, 6X, 4HGPPW, 6X, 2HDW/ 1H)

```

```

C **** BEGINNING OF LOOP TO GENERATE NEW INITIAL FP AND GP PROFILES ****
DO 399 LOOP=1, KMI
WRITE (6,98)
C **** BEGINNING OF INNER LOOP FOR FP PROFILE ****
DO 349 LOOPF=1, KMI
IF (MOP.LT.C) GO TO 305
C **** FOR VARIABLE PROPERTY FLOW, RECALCULATE D AND DP ****
B1=TF(I)-1.
DO 304 J=1, JY
FV=1.-FP(J)
D(J)=2.*TF(I)*(1.-BH*GP(J))/(1.+SQRT(1.+4.*B1*FV*FV*TF(I)
1 * (1.-BH*GP(J)))) (II-16)
DP(J)=(2.*B1*D(J)*D(J)*FV*FPP(J)-TF(I)*BH*GPP(J)
1 / (1.+2.*B1*D(J)*FV*FV)
DB(J)=(P*(SHR-1.)*M(I)*M(I)*TF(I)
1 + (1.-BH*GP(J)-D(J)*D(J)*FV*FV)
2 + (SHR-1.)*M(I)*M(I)*C(J)*D(J)*FV*GAMX*(FP(J)+Y(J)*FPP(J))
3 -TF(I)*BH*(STRX*GP(J)+GAMX*GPP(J)*Y(J))
4 / (1.+ (SHR-1.)*M(I)*M(I)*D(J)*FV*FV) (II-32,42)
304 CONTINUE
305 CONTINUE
C **** SET PARAMETERS FOR EITHER LAMINAR OR TURBULENT FLOW ****
GO TO (315,320,321,310,315,320,321), IOP
310 CONTINUE
C **** SET P*, Q* AND R* ****
C=F(JE)*C
P=C*C*RL*BS (II-29a)
Q=P*(1.-MI*MI)+C*C*RL*(1.-BS)/2. (II-29b)
VP=VW(I)/U(I)*C*RL
IF (IABS(DOP).EQ.1) VP=VP/D(1)
RDT(2)=C*RL
RDF=RDT(2)
CA=0.0
R=0.0
IF (ABS(RW(2)/(X(2)-X(1))),LT.1.E-8) GO TO 313
R=RL*C*C*(RW(3)-RW(1))/(X(3)-X(1))*X(2)-X(1)/(RW(3)+RW(1)) (II-29c)
CA=2.*OI*COAI*C*(X(2)-X(1))/RW(2)
DO 312 J=1, JY
Y(J)=YY(J)*(1.+YY(J)*CA/4.)
312 CONTINUE
313 CONTINUE
OR=O+R
GO TO 330
315 CONTINUE
FPP(1)=FPP(1)*F(JE)
CF(I)=2.*TAU(I)
VP=VW(I)/U(I)*RDT(I)
IF (IABS(DOP).EQ.1) VP=VP/D(1)
GO TO 325
320 CONTINUE
C **** SET P AND Q ****
P=-TAU(1)*BS
321 CONTINUE
CF(I)=2.*TAU(1)
GAM=SQRT(ABS(TAU(1)))
GAMX=-GAM/SK*(C+CMU*P) (II-34)
IF (GAM.GT.ZERC) STRX=- (GAM+STR(I)/GAM)/SK*(Q+CMU*P) (II-37)
VP=VW(I)/U(I)
IF (IABS(DOP).EQ.1) VP=VP/D(1)
325 CONTINUE
DO 326 J=1, JE
VH(J)=((R*D(J)*(Y(J)-F(J))+GAM/SK*CMU*P*Y(J)*D(J)-VP)*FPP(J)
1 + (R*DP(J)*(Y(J)-F(J))- (P*D(J)+DB(J))* (2.-FP(J))
2 + (1.-FP(J))*(D(J)-Y(J)*DP(J))*GAM/SK*CMU*P-VP*DP(J))*FP(J)
3 +R*DP(J)*F(J)+P*(D(J)-1.)*R*Y(J)*DP(J)+DB(J)+VP*DP(J))
VHP(J)=(D(J)*(Y(J)-F(J))+GAM/SK*Y(J)*D(J))*FPP(J)
1 + (DP(J)*(Y(J)-F(J))
2 + (1.-FP(J))*(D(J)-Y(J)*DP(J))*GAM/SK)*FP(J)
3 - (Y(J)-F(J))*DP(J)
326 CONTINUE
CALL INTEG (JE, JD, Y, VH, C, VH)
CALL INTEG (JE, JD, Y, VHP, C, VHP)
Q=- (CF(I)/2.*RDF+VH(JE)/F(JE))/VHP(JE)*F(JE) (II-41)

```



```

OR=Q+R
330 CONTINUE
C **** CALCULATE VE* OR VE ****
CALL VIS (JE, JY, JD, YY, FP, FPP, GP, GPP, D, DP, TAU, VH, VHP,
1 TURB(I), SW(I), CW(I), SHR, BH, STC, TO, TF(I), RDT(I), DT(I),
2 F(JY), PR, PRT, JK, VE, VEG)
C **** IF INPUT PROFILES ARE CORRECT, SKIP FP RECALCULATION ****
IF (IOP.LE.3) GO TO 350
C **** CALCULATE CCEFFICIENTS AND CALL $PROFYL FOR SOLUTION ****
FPPW=FPP(1)
FPE=0.0
DO 335 J=1, JY
CQ=OR*(Y(J)-F(J))-VP
B(J,1)=CQ*DP(J)-(P*D(J)+DB(J))*(2.-FP(J))
1 - (1.-FP(J))*D(J)-Y(J)*DP(J)*GAMX
B(J,2)=(CQ-Y(J)*GAMX)*E(J)
B(J,3)=-CQ*DP(J)+P*(D(J)-1.)+DB(J)
B(J,4)=- (1.+CA*Y(J))*VE(J)*RDF
B(J,5)=-DP(J)/D(J)*(1.-FP(J))
335 CONTINUE
CALL PROFYL (JEP, JY, JE, Y, B, ET, 1.0, FPPW, FPE, 2,
1 FP, VH, VHP, VHPP)
JE=MAXC (JEP, JEG)
C **** CALCULATE TAU AND SF ****
JM=1
JYM=JY-1
DO 340 J=1, JYM
FPP(J)=(FP(J+1)-FP(JM))/(Y(J+1)-Y(JM))
JM=J
TAU(J)=VE(J)*(IP(J)/D(J)*(1.-FP(J))-FPP(J))*SQRT(1.+CA*Y(J))
VH(J)=(1.-FP(J))*(1.-D(J)*(1.-FP(J)))
340 CONTINUE
FPP(JY)=0.0
TAU(JY)=0.0
VH(JY)=0.0
CALL INTEG (JE, JD, Y, FP, 0.0, F)
CALL INTEG (JE, JD, Y, VH, 0.0, VH)
SF(I)=F(JE)/VH(JE)
C **** PRINT OUT INTERMEDIATE FP PARAMETERS AND VARIABLES ****
WRITE (6,72) JK, JEP, F(JEP), FPP(1), SF(I), P, Q, R
72 FORMAT (1X, 1HF, 2(1X, I3), 6(1X, 1PE9.2))
C **** TEST FOR CONVERGENCE OF FP ****
IF (LOOPF.GT.1.AND.ABS(F(JE)-1.).LT.XT) GO TO 350
349 CONTINUE
C **** END OF INTERMEDIATE LOOP FOR FP PROFILE ****
350 CONTINUE
C **** SET BOUNDARY CCNDITICNS CN GP OR GPP ****
IBC=IABS(MOP)
GO TO (400, 351, 352), IBC
351 CONTINUE
GPW(I)=GBC(I)
GPPW=GPP(1)
STR(I)=-GPPW/D(1)*VEG(1)
GO TO 353
352 CONTINUE
GPW(I)=GP(1)
GPPW=-GBC(I)*D(1)/VEG(1)
STR(I)=GBC(I)
IF (IOP.NE.4) GO TO 353
GPPW=GPPW*C*RL
STR(I)=GBC(I)/C/RL
353 CCNTINUE
C **** IF INPUT PECFILES ARE CORRECT, SKIP GP RECALCULATION ****
IF (IOP.LE.3) GO TO 410
C **** CALCULATE COEFFICIENTS AND CALL $PROFYL FOR GP SOLUTION ****
GPE=0.0
DO 360 J=1, JY
B(J,1)=- (1.-FP(J))*STRX
B(J,2)=OR*(Y(J)-F(J))-VP-GAMX*Y(J)
E(J,3)=0.0
B(J,4)=- (1.+CA*Y(J))*VEG(J)/D(J)*RDF
B(J,5)=- (SHR-1.)*M(1)*M(1)/BH/TF(1)*(VE(J)/VEG(J)-1.)
1 *D(J)*(1.-FP(J))*(DF(J)*(1.-FP(J))-D(J)*FPP(J))

```

(III-11)

(III-12)

```

360 CONTINUE
1 CALL PROFYL (JEG, JY, JD, Y, B, ET, GPW(I), GPPW, GPE, IBC,
GP, VH, VHP, VHPP)
JE=MAXO (JEF, JEG)
JH=1
JYM=JY-1
DO 365 J=1, JYM
GPP(J) = (GP(J+1) - GP(JM)) / (Y(J+1) - Y(JM))
JH=J
365 CCONTINUE
IF (IBC.EQ.3) GPP(1)=GPPW
C **** PRINT OUT INTERMEDIATE GP PARAMETERS AND VARIABLES ****
WRITE (6,76) JEG, GP(1), GPP(1), D(1)
76 FORMAT (1X, 1HG, 5X, 1S, 3(1X, 1PE9.2))
C **** IF FLOW HAS CONSTANT FLUID PROPERTIES, LEAVE LOOP ****
IF (MOP.LT.0) GO TO 40C
C **** TEST GP OR GPP FOR CONVERGENCE ****
IF (LOOP.LT.2) GO TO 399
IF (ABS(GPW(I)).GT.ZERO) GO TO 396
IF (ABS(GP(1)-GPW(I)).LT.ZERO) GO TO 397
GO TO 399
396 CONTINUE
IF (ABS((GP(1)-GPW(I))/GP(I)).GT.XT) GO TO 399
397 CONTINUE
IF (ABS(GPPW).GT.ZERO) GO TO 398
IF (ABS(GPP(1)-GPPW).LT.ZERO) GO TO 400
GO TO 399
398 CONTINUE
IF (ABS((GPP(1)-GPPW)/GPPW).LT.XT) GO TO 400
399 CONTINUE
400 CONTINUE
GO TO 415
C **** PRINT OUT PARAMETERS (IF INPUT PROFILES ARE UNCHANGED) ****
WRITE (6,72) JK, JEF, F(JEF), FPP(1), SF(I), P, Q, R
72 FORMAT (6,76) JEG, GP(1), GPP(1), D(1)
415 CONTINUE
IXF=2
GO TO (425,430,43C,420,425,430,430), IOP
C **** CONTINUE
FOR OPTION 4, CALCULATE DT(2), EDT(2) AND PRINT EXPLANATION ****
IXF=3
I=2
SF(1)=SF(2)
DT(2)=(X(2)-X(1))*SORT(Q/RL/(BS*(1.-ML*ML)+(1.-BS)/2.))
EDT(2)=RL*DT(2)/(X(2)-X(1))
IF (ABS(BS-1.J).LT.ZERO) DT(1)=DT(2)
MT(1)=D(1)/SF(1)
78 FORMAT (1HG, 29HTHE FOLLOWING PROFILE AT X = , F10.5, 1X,
1 31HIS A STARTING LAMINAR PROFILE. THE PROFILE AT
2 45HIT IS TAKEN TO BE IDENTICAL TO THE PROFILE AT/
3 1X, 4HX = , F10.5, 11HWHERE DT = , 1PE9.2)
C 425 CONTINUE
FOR LAMINAR FLOW, RESCALE P*, Q*, E* AND VP* ****
P=P/RDT(I)
Q=Q/RDT(I)
R=R/RDT(I)
CR=QR/RDT(I)
VP=VP/RDT(I)
C 430 CONTINUE
CALCULATE DTX, MT, CF, HT AND ST ****
DTXM=Q-P*(1.-M(I))*M(I)
MT(I)=DT(1)/SF(I)
CF(I)=2.*TAU(1)
B1=GPW(I)-(TF(I)-1.)/BH/TF(I)
ST(I)=0.
IF (ABS(B1).GT.ZERO) ST(I)=STR(I)/B1
DO 44C J=1, JE
VHPP(J)=GP(J)*(1.-FP(J))
440 CONTINUE
CALL INTEG (JE, JD, Y, VHPP, (.J), VHPP)
HT(I)=VHPP(JE)*IT(I)

```

```

IF (IOP.NE.4) GO TO 45C
HT(1)=HT(2)
NU=RL*PR*ST(2)
WRITE (6,79) X(1), NU
79 FORMAT (1X, 26HTHE NUSSELT NUMBER AT X = , 1PE9.2, 4H IS , 1PE9.2)
450 CONTINUE
C **** PRINT PROFILES AND PARAMETERS WITH $FILE ****
WRITE (6,99)
CALL FILE (LABEL, I, YY, F, FP, FPP, GP, GPP, D, DP,
1 VH, VHP, VHEP, TAU, VE, VEG, SHR, BH, PR, PRT,
2 X, U, M, TUEB, RW, VW, SW, CW,
3 RDT, DI, MT, HT, SP, CP, ST, STR, ID, JE, JY, JD, JDIV)
IF (IX-I.LE.C) STOP
EX=0.0
DO 480 J=1, JY
FB(J)=F(J)
FPB(J)=FP(J)
GPB(J)=GP(J)
DB(J)=D(J)
480 CONTINUE
C **** END OF INITIALIZATION, BEGINNING OF FORWARD MOTION IN X ****
C
DO 899 I=IXF, IX
IXA=I
C **** MOVE FP, GP AND D BACK TO MOVE FORWARD IN X ****
DO 510 J=1, JY
FBB(J)=FB(J)
FB(J)=F(J)
FPBB(J)=FPB(J)
FPB(J)=FP(J)
FPPB(J)=FPP(J)
GPBB(J)=GPB(J)
GPPB(J)=GPP(J)
GPB(J)=GP(J)
DBB(J)=DB(J)
DB(J)=D(J)
DPB(J)=DP(J)
510 CONTINUE
JEB=JE
CAB=CA
PB=P
RB=R
IB=I-1
DXB=DX
DX=X(I)-X(IB)
DT(I)=DT(IB)+DTXM*DX
DTBB=DT(IB)
IF (IB.GT.1) DTBB=DT(I-2)
VPB=VW(IB)/U(IE)
IF (IABS(DOP).EQ.1) VPE=VPB/DB(1)
IF (I.GE.IX) GC TO 520
RX=U(I-1)/U(I)*(X(I)-X(I+1))/(X(I-1)-X(I))/(X(I-1)-X(I+1))
1 + (2.*X(I)-X(I-1)-X(I+1))/(X(I)-X(I-1))/(X(I)-X(I+1))
2 + U(I+1)/U(I)*(X(I)-X(I-1))/(X(I+1)-X(I-1))/(X(I+1)-X(I))
CA1=C.0;
IF (ABS(RW(I)/IT(I)).LT.0.1) GO TO 520
RX=RW(I-1)/RW(I)*(X(I)-X(I+1))/(X(I-1)-X(I))/(X(I-1)-X(I+1))
1 + (2.*X(I)-X(I-1)-X(I+1))/(X(I)-X(I-1))/(X(I)-X(I+1))
2 + RW(I+1)/RW(I)*(X(I)-X(I-1))/(X(I+1)-X(I-1))/(X(I+1)-X(I))
CA1=2.*CI*SQRT(1.-RX*RW(I)*RX*RW(I))/RW(I)
520 CONTINUE
C **** PRINT INPUT PARAMETERS FOR NEXT X STATION ****
WRITE (6,51) (IABPI(K), K=1, 18)
WRITE (6,60) X(I), U(I), M(I), TURB(I), GBC(I), RW(I), VW(I),
1 SW(I), CW(I)
WRITE (6,70)
WRITE (6,81)
81 FORMAT (1HC, 1HF, 2X, 2HJK, 1X, 3HJEF, 5X, 3HFJE, 6X, 4HFPPW, 6X,
1 2HDT, 7X, 4HDTXM, 7X, 2HPM, 8X, 2HQM, 8X, 2HRM/

```

```

2 1X, 1HG, 5X, 3HJEG, 5X, 3HGFV, 6X, 4HGPPW, 6X, 2HDW/ 1HQ)
C **** BEGINNING OF ITERATIVE LOOP TO CALCULATE FP AND GP PROFILES ****
DO 799 LOOP=1, KMI
WRITE (6,98)
C **** BEGINNING OF INNER LOOP TO CALCULATE FP PROFILE ****
DO 670 LOOPF=1, KMI
C **** RECALCULATE DT, RDT, P, Q, AND R ****
DT(I)=TI(I)*F(JE)
RDT(I)=RDT(IB)*U(I)/U(IB)*DT(I)/DT(IB)
1 *(TF(I)/TF(IB))**((1.5-1.)/(SHR-1.))
2 *(1./TF(I)+STC/TG)/(1./TF(IB)+STC/TG)
DTXM=(DT(I)-DT(IB))/DX
DTXB=(DT(I)-DT(IB))/(DX+DXB)
P=DT(I)*UX
PM=(P+PB)/2.
QM=DTXM+PM*(1.-(0.5*(M(I)+M(IB))))**2)
QB=DTXB+PB*(1.-M(IB)*M(IB))
R=RX*DT(I)
RM=(R+RB)/2.
ORM=QM+RM
ORB=QB+RB
CA=CA1*DT(I)
IF (ABS(RM(I)/DT(I)).LT.0.1) GO TO 606
DO 605 J=1, JY
YY(J)=2.*Y(J)/(1.+SQRT(1.+CA*Y(J)))
605 CONTINUE
606 CONTINUE
IF (MOP.LT.0) GO TO 611
C **** RECALCULATE VE, D AND DP ****
B1=TF(I)-1.
DO 610 J=1, JY
FV=1.-FP(J)
D(J)=2.*TF(I)*(1.-BH*GP(J))/(1.+SQRT(1.+4.*B1*FV*FV*TF(I))) (II-16)
1 *(1.-BH*GP(J))
DP(J)=(2.*B1*D(J)*D(J)*FV*FPP(J)-TF(I)*BH*GPP(J))
1 / (1.+2.*B1*D(J)*FV*FV)
610 CONTINUE
611 CONTINUE
CALL VIS (JE, JY, JD, YY, FP, FPP, GP, GPP, D, DP, TAU, VH, VHP,
1 TURB(I), SW(I), CW(I), SHP, BH, STC, T, TF(I), RDT(I), DT(I),
2 F(JY), PE, FRT, JK, VE, VEG)
C **** CALCULATE FE COEFFICIENTS AND CALL $PROFYL FOR FP SOLUTION ****
DTM=(DT(I)+DT(IB))/2.
VPM=(VW(I)+VW(IB))/ (U(I)+U(IB))
IF (ABS(DCP).EQ.1) VPM=VPM*2./ (D(1)+DB(1))
FPE=.
FPPW=FPP(1)
DO 650 J=1, JY
FPM=(FP(J)+FEB(J))/2.
DM=(D(J)+DB(J))/2.
LPM=(DP(J)+DPB(J))/2.
DDXM=(D(J)-DE(J))/DX
DDXB=(D(J)-DEB(J))/(DX+DXB)
C1=ORM*(Y(J)-(F(J)+FB(J))/2.)-VPM-DTM*(F(J)-FB(J))/DX
C1=C1*DM
C2=C1*DPM-(PM*DM+DTM*DDXM)*(2.-FPM)
C3=-C1*DPM+PM*(DM-1.)+DTM*DDXM
C4=DM*(1.-FPM)*ETM/DX
C1B=ORB*(Y(J)-FB(J))-VFB-DT(IB)*(F(J)-FBB(J))/(DX+DXB)
C1B=C1B*DB(J)
C2B=C1B*DPB(J)-(PB*DB(J)+DT(IB)*DDXB)*(2.-FPB(J))
C3B=-C1B*DPB(J)+PE*(DB(J)-1.)+DT(IB)*DDXB
C4B=(1.-FPB(J))*DB(J)*ET(IB)/(DX+DXB)
B(J,1)=C2-2.*C4+C4B
E(J,2)=C1
B(J,3)=2.*C3-C1B+(C1-C1B)*FPPB(J)+(C2+2.*C4-C2B)*FPP(J)
1 -C4B*FPPB(J)
B(J,4)=- (1.+CA*Y(J))*VE(J)
B(J,5)=-DP(J)/D(J)*(1.-FP(J)) (III-9)
650 CONTINUE
CALL PROFYL (JEF, JY, JD, Y, B, ET, 1.0, FPPW, FPE, 2,
1 FP, VH, VHP, VHPP)
JE=MAX0 (JEF, JEG)

```

```

C **** CALCULATE TAU ****
  JYM=JY-1
  JM=1
  DO 660 J=1, JYM
    FPP(J)=(FP(J+1)-FP(JM))/(Y(J+1)-Y(JM))
    JM=J
    TAU(J)=VE(J)*(DP(J)/D(J)*(1.-FP(J))-FPP(J))*SQRT(1.+CA*Y(J))
660 CONTINUE
    FPP(JY)=0.0
    TAU(JY)=0.0
    VH(JY)=0.0
    CALL INTEG (JE, JD, Y, FP, J.C, F)
C **** PRINT OUT INTERMEDIATE FP PARAMETERS AND VARIABLES ****
  WRITE (6,82) JK, JEF, F(JEF), FPP(1), DT(I), DTXM, PM, QM, RM
82 FORMAT (1X, 1HF, 2(1X, I3), 7(1X, 1PE9.2))
C **** TEST FOR FATAL ERROR ****
  IF (F(JEF).LT.C.C.CR.F(JEF).GT.10.0) GO TO 901
C **** TEST F AND FFP FOR CONVERGENCE ****
  IF (LOOP.EQ.1) GO TO 670
  IF (ABS((FPP(1)-FPPW)/FPPW).GT.XT) GO TO 670
  IF (ABS(F(JE)-1.).LT.XT) GO TO 750
670 CONTINUE
C **** END OF INNER LOOP TO CALCULATE FP PROFILE ****
750 CONTINUE
C **** SET BOUNDARY CONDITIONS ON GP OR GPF ****
  IBC=IABS(MOP)
  GO TO (800,751,752), IEC
751 CONTINUE
  GPW(I)=GBC(I)
  GPPW=GPP(1)
  STR(I)=-GPPW/D(1)*VEG(1)
  GO TO 753
752 CONTINUE
  GPW(I)=GP(1)
  GPPW=-GBC(I)*D(1)/VEG(1)
  STR(I)=GBC(I)
753 CONTINUE
C **** CALCULATE GP COEFFICIENTS AND CALL $PROFYL FOR GP SOLUTION ****
  GPE=0.0
  DO 760 J=1, JY
    C7=ORM*(Y(J)-(F(J)+FB(J))/2.)-DTM*(F(J)-FB(J))/DX-VPM
    C8=(1.-(FP(J)+FPB(J))/2.)*DTM/DX
    C7B=ORB*(Y(J)-FE(J))-VEB-DT(IB)*(F(J)-FBB(J))/(DX+DXB)
    C8B=(1.-FPB(J))*DT(IB)/(DX+DXB)
    E(J,1)=-2.*C8+C8B
    B(J,2)=C7
    B(J,3)=(C7-C7B)*GPPB(J)+2.*C8*GPB(J)-C8B*GPBB(J)
    B(J,4)=- (1.+CA*Y(J))*VEG(J)/D(J)
    B(J,5)=- (SHR-1.)*M(I)*M(I)/PH/TF(I)*(VE(J)/VEG(J)-1.)
    1 *D(J)*(1.-FP(J))*(DP(J)*(1.-FP(J))-D(J)*FPP(J))
760 CONTINUE
  CALL PROFYL (JEG, JY, JE, Y, B, ET, GPW(I), GPPW, GPE, IBC,
  1 GP, VH, VHP, VHPP)
  JE=MAXC(JEF,JFG)
  JM=1
  JYM=JY-1
  DO 765 J=1, JYM
    GPP(J)=(GP(J+1)-GP(JM))/(Y(J+1)-Y(JM))
    JM=J
765 CONTINUE
    IF (IBC.EQ.3) GPP(1)=GPEW
C **** PRINT INTERMEDIATE GP PARAMETERS AND VARIABLES ****
  WRITE (6,86) JEG, GP(1), GPP(1), D(1)
86 FORMAT (1X, 1HG, 5X, I3, 3(1X, 1PE9.2))
C **** IF FLOW HAS CONSTANT FLUID PROPERTIES, LEAVE LOOP ****
  IF (MOP.LT.C) GO TO 800
C **** TEST GP OF GPE FOR CONVERGENCE ****
  IF (LOOP.EQ.1) GO TO 799
  IF (ABS(GPW(I)).GT.ZERO) GO TO 796
  IF (ABS(GP(1)-GPW(I)).LT.ZERO) GO TO 797
  GO TO 799
796 CONTINUE
  IF (ABS((GP(1)-GPW(I))/GP(I)).GT.XT) GO TO 799

```

```

797 CONTINUE
IF (ABS(GPPW).GT.ZERO) GO TO 798
IF (ABS(GPP(1)-GPPW).LT.ZERO) GO TO 800
GO TO 799
798 CONTINUE
IF (ABS((GPP(1)-GPPW)/GPPW).LT.XT) GO TO 800
799 CONTINUE
C **** END OF ITERATIVE LOOP TO CALCULATE FP AND GP PROFILES ****
800 CONTINUE
C **** COMPUTE SF, MI, HT, CF AND ST ****
DO 840 J=1, JE
FV=1.-FP(J)
VHP(J)=FV*(1.-I(J)*FV)
VHPP(J)=GP(J)*FV
840 CONTINUE
CALL INTEG (JE, JD, Y, VHP, 0.0, VHP)
CALL INTEG (JE, JD, Y, VHPP, 0.0, VHPP)
SF(I)=1./VHP(JF)
MT(I)=DT(I)/SF(I)
HT(I)=VHPP(JE)*DT(I)
CF(I)=2.*TAU(1)
STR(I)=-VEG(1)*GPP(1)/E(1)
B1=GPW(I)-(TF(I)-1.)/BH/TF(I)
ST(I)=0.0
IF (ABS(B1).GT.ZERO) ST(I)=STR(I)/B1
C **** CALCULATE INTEGRAL OF MOMENTUM AND THERMAL ENERGY EQUATIONS ****
HB=(SF(I)+SF(IE))/2.
COF1=(U(I)/U(IE))**(2.+HB)*(TF(IE)/TF(I))**(1./(SHR-1.))
1 *MT(I)/MT(IE)
IF (RW(IE)/DT(IE).GT.0.1) COF1=COF1*RW(I)/RW(IE)
COF2=EXP(DX*((CF(IE)+CF(I))/2.+2.*VPM)/(MT(IE)+MT(I))) (II-21)
COG1=1.0
IF (ABS(HT(IE)).GT.ZERO) COG1=U(I)/U(IE)
1 * (TF(IE)/TF(I))**(1./(SHR-1.))*HT(I)/HT(IE)
IF (RW(IE)/DT(IE).GT.0.1) COG1=COG1*RW(I)/RW(IE)
COG2=1.0
B1=0.0
E2=HT(I)+HT(IE)
IF (ABS(B2).GT.ZERO) B1=(STR(I)+STR(IE)+VPM*(GP(1)+GP(IE)))*DX/B2
IF (ABS(E1).LT.98.0) CCG2=EXP(B1) (II-23)
CMTF=CMTF*COF2/COF1
CMTG=CMTG*COG2/COG1
C **** PRINT RESULTS AS AN INDICATION OF ACCURACY ****
WRITE (6,89) CCF1, COF2, COG1, COG2
89 FORMAT (1H0, 9X, 42HINTEGRALS OF MOMENTUM AND ENERGY EQUATIONS
1 //18X, 8HMOENTUM, 26X, 6HENERGY/
2 //13X, F7.4, 4H = , F7.4, 16X, F7.4, 4H = , F7.4)
C **** RESET MT, DT, HT, AND RDT TO MATCH CF ****
DTS=DT(I)
MT(I)=MT(I)*COF2/COF1
DT(I)=SF(I)*MT(I)
RDT(I)=RDT(I)/DTS*DT(I)
HT(I)=HT(I)*DT(I)/DTS
DTXM=(DT(I)-DT(IE))/DX
C **** PRINT PROFILES AND PARAMETERS WITH $FILE ****
WRITE (6,99)
CALL FILE (LABEL, I, YY, F, FP, FPP, GP, GPP, D, DP,
1 VH, VHP, VHPP, TAU, VF, VEG, SHR, BH, PR, PRT,
2 X, U, M, TURB, RW, VW, SW, CW,
3 RDT, DT, MT, HT, SF, CF, ST, STR, ID, JE, JY, JD, JDIV)
899 CONTINUE
C **** END OF FORWARD MOTION IN X ****
GO TO 905
901 CONTINUE
C **** PRINT PROFILES AND PARAMETERS WHICH CONTAIN FATAL ERROR ****
WRITE (6,99)
CALL FILE (LABEL, I, YY, F, FP, FPP, GP, GPP, D, DP,
1 VH, VHP, VHPP, TAU, VF, VEG, SHR, BH, PR, PRT,
2 X, U, M, TURB, RW, VW, SW, CW,
3 RDT, DT, MT, HT, SF, CF, ST, STR, ID, JE, JY, JD, JDIV)
905 CONTINUE
C **** PRINT OUT SUMMARY OF PRINCIPAL BOUNDARY LAYER PARAMETERS. ****
WRITE (6,90) (LABEL(K), K=1,18)

```

```

WRITE (6,91)
DO 910 I=1, IXA
WRITE (6,92) X(I), DT(I), MT(I), HT(I), SF(I), CF(I), ST(I),
1 GPW(I), RCT(I), U(I), M(I), TURB(I), RW(I), VW(I), SW(I), CW(I)
910 CONTINUE
WRITE (6,99)
GO TO 100
99 FORMAT (//45X, 39HPRINCIPAL BOUNDARY LAYER PARAMETERS FOR/
1 26X, 18A4)
91 FORMAT (//5X, 1HX, 8X, 2HDT, 7X, 2HMT, 7X, 2HHT, 5X,
1 2HSP, 5X, 2HCF, 6X, 2HST, 7X, 3HGPW, 5X,
2 3HPDI, 7X, 1HU, 7X, 1HM, 4X, 4HTURB, 5X, 2HRW,
3 8X, 2HVV, 7X, 2HSW, 4X, 2HCW/)
92 FORMAT (/1X, F8.5, 1X, 3(F8.6, 1X), F5.3, 1X,
1 2(F7.5, 1X), F8.5, 1X, F8.4, 1X, F8.3, 1X,
2 F6.3, 1X, F5.3, 1X, F8.3, 1X, F9.4, 1X, F8.5, 1X, F5.1)
END

```

## Description of the Subroutines

Subroutine VIS calculates the effective viscosity and effective conductivity in terms of the local flow variables. The entire effective viscosity hypothesis for turbulent flow is contained in this subroutine so that changes can be made without affecting the main program.

In laminar flow  $T$  is merely  $\nu(\eta)/U\delta^*$  and  $T_g$  is  $\nu(\eta)/U\delta^*P_r$ . In turbulent flow given by

$$T = \frac{\delta^* k}{\delta^*} \left[ \frac{\phi(\tilde{X}R)}{\tilde{R}} + \Phi(X) - X \right], \quad (IV-1a)$$

and

$$T_g = \frac{\nu/\nu_\infty}{R_{\delta^*} P_r} + \frac{1}{P_{rt}} \left[ T - \frac{\nu/\nu_\infty}{R_{\delta^*}} \right], \quad (IV-1b)$$

where  $X = \kappa y \sqrt{\tau(\eta)/\bar{\rho}(\eta)}/U\delta_k^* + y_s/\delta_k^*$ . The form of the functions and is shown in Figure 2. A more complete discussion of this hypothesis is given in Reference [2].

A functional method of simulating the effects of wall roughness in turbulent flow is provided which is completely contained in  $\$VIS$ . Essentially, this method consists of beginning the calculation ( $y = 0$ ) at a point  $s_w$ , the effective wall roughness size used by Nikuradse [15], further out on the effective viscosity function than would be the case for a smooth wall. The resulting "law of the wall" velocity profile then has the experimentally observed behavior as a function of effective roughness size. When the roughness size is large the logarithmic portion of the velocity profile is simply displaced downward proportional to  $\log s_w u_\tau/\nu$ . As the roughness is reduced, the correct departure from this behavior is achieved with an empirical relation.

A correction to the effective viscosity is also provided for the influence of longitudinal wall curvature. This correction is obtained through an application of the method used in Reference [16] to compressible flow. The basic assumption is the advection and convection terms in



equations (27-30) in Reference [17] are negligible. The result is a set of four algebraic equations involving the turbulent shear stress and the three components of turbulent energy. This set can then be solved to yield an expression for the effective viscosity correction. The correction takes the form,

$$v_c = \left[ \frac{1 - c_u \left( 1 + \frac{\overline{\rho v' u'}}{\rho u' v'} \right)}{1 - c_u} \right]^{1/2} \left\{ 1 - 4.0 \frac{c_u (1+c_u) \left( 1 + \frac{\overline{\rho v' u'}}{4 \rho u' v'} \right)}{\left[ 1 - c_u \left( 1 + \frac{\overline{\rho v' u'}}{\rho u' v'} \right) (1-c_u) \right]} \right\}^{3/2} |1-c_u|, \quad (IV-2)$$

where the terms  $\overline{(\rho'v'u)}/(\rho u'v')$  is evaluated using Reynolds analogy,

$$\frac{\overline{\rho'v'u}}{\rho u'v'} = \frac{u}{h} \frac{1}{P_{rt}} \frac{(\partial h/\partial y)}{(\partial u/\partial y)} \quad (IV-3)$$

Finally, a very minimal mechanism for causing transition is provided, again entirely within this subroutine. This mechanism allows the user to specify the relative proportions of laminar and turbulent kinematic viscosity which will prevail according to the relation

$$T = T_{\text{turbulent}} + (1 - T) T_{\text{laminar}}, \quad (0 < T < 1) \quad (IV-4)$$

In complete laminar flow  $T = 0$  and in fully turbulent flow  $T = 1$ .

#### Classification of Arguments

Inputs: JE, JY, JD, YY, FP, FPP, GP, GPP, D, DP, TAU, VH, VHP, TURB, SW, CW, SHR, BH, STC, TO, TF, RDT, DT, FJE, PR, PRT.

Outputs: JK, VE, VEG.

```

SUBROUTINE VIS (JE, JY, JD, YY, FP, FPP, GP, GPP, D, DP, TAU,
1  VH, VHP, TURB, SW, CW, SHR, BH, STC, TO, TF, RDT, DT, FJE,
2  PR, PRT, JK, VE, VEG)
DIMENSION YY(JL), FP(JD), FPP(JD), GP(JD), GPP(JD), D(JD), DP(JD)
DIMENSION TAU(JL), VH(JL), VHP(JD), VE(JD), VEG(JD)
DATA SIG3, SK, BK/ 328.51, 0.41, 0.016/
DATA ZERO/ 1.0E-10/
JK=JE
DO 100 J=1, JY
VH(J)=D(J)**2.5*(1./TF+STC/TC)/(D(J)/TF+STC/TO)
100 CONTINUE
IF (TURB.LT.ZERO) GO TO 400
DO 120 J=1, JE
VHP(J)=1.-b(J)*(1.-FP(J))
120 CONTINUE
CALL INTEG (JE, JD, YY, VHP, 0.0, VHP)
VR=VHP(JE)/FJE*BK
GAM=SQRT (ABS (TAU(1)) *D(1))
YPS=SW/DT*RDT/VH(1)*GAM/30.0
1  * (1.0+3.0*EXP (-SW/DT*RDT/VH(1)*GAM/150.0))
DO 200 J=1, JY
JK=J
CHI=SK*(RDT/VH(J)*YY(J)*SQRT (D(J)*ABS (TAU(J))))+YPS
CHI3=CHI*CHI*CHI
VF(J)=VH(J)*(1.+CHI3*CHI/(CHI3+SIG3))/RDT
VEG(J)=VE(J)/PRT+VH(J)*(1./PR-1./PRT)/RDT
VHP(J)=1.0
IF (VE(J).GT.VR) GO TO 210
200 CCNTINUE
GO TO 300
210 CONTINUE
DO 220 J=JK, JY
VE(J)=VR
VEG(J)=VR/PRT
VHP(J)=1.0
220 CONTINUE
300 CCNTINUE
IF (ABS (CW).LT.ZERO) GO TO 370
DO 310 J=1, JY
VHP(J)=0.0
FPPV=DP(J)*(1.-FP(J))-D(J)*FPP(J)
IF (ABS (FPPV).LT.ZERO) GO TO 310
FPV=D(J)*(1.-FP(J))
BM=(TF-1.)/IF
CU=(DT/CW)*FPV/FPPV
B1=1.-CU
DC=-FPV/FPPV*(EH*GPP(J)+2.*BM*FPPV*FPV)
1 / (1.-BH*GE(J)-BM*FPV*FPV)/PRT
B2=1.-CU*(1.+DC)*B1
IF (ABS (B1*B2).LT.ZERO) GO TO 310
B3=1.-CU*(1.+DC)
B4=(1.-CU*(1.+DC))/B1
IF (B4.LT.ZERO) GO TO 310
B5=1.-4.* (1.+CU)*(1.+DC)*CU/B2
IF (B5.LT.ZERO) GO TO 310
VHP(J)=SQRT (E4)*B5**1.5*ABS (B1)
310 CONTINUE
370 CONTINUE
DO 380 J=1, JY
VE(J)=TURB*VHP(J)*(VE(J)-VH(J)/RDT)+VH(J)/RDT
VEG(J)=TURB*VHP(J)*(VEG(J)-VH(J)/PR/RDT)+VH(J)/PR/RDT
380 CONTINUE
RETURN
400 CONTINUE
DO 420 J=1, JY
VE(J)=VH(J)/RDT
VEG(J)=VE(J)/PR
420 CONTINUE
RETURN
END

```

(11-18)

(IV-1b)

Subroutine PROFYL controls the numerical solution of the ordinary differential equations in the form of (III-7) and (III-8) as described in Section III.

Classification of Arguments

Inputs: JE, JY, JD, Y, B, ET, FPW, FPPW, FPE, IBC.

Outputs: FP, VH, VHP, VHPP.

```

SUBROUTINE PROFYL (JE, JY, JD, Y, B, ET, FPW, FPPW, FPE, IBC,
1  FP, VH, VHP, VHPP)
DIMENSION Y (JE), B (JD, 5)
DIMENSION FP (JD), VH (JD), VHP (JD), VHPP (JD)
JE=JY
VHPP (1)=0.0
VH (1)=0.0
VHP (1)=FPW
IF (IBC.NE.3) GO TO 100
VH (1)=1.0
VHP (1)=- (FPPW+E (1, 5)) * (Y (2)-Y (1))
100 CONTINUE
JYM=JY-1
DO 200 J=2, JYM
VHPP (J)=VHPP (J-1) + (B (J, 5) + B (J-1, 5)) / 2. * (Y (J) - Y (J-1))
DY=Y (J+1) - Y (J-1)
ATP=- (B (J+1, 4) + B (J, 4)) / (Y (J+1) - Y (J)) / DY
ATM=- (B (J, 4) + B (J-1, 4)) / (Y (J) - Y (J-1)) / DY
A1=ATM-B (J, 2) / DY
A2=ATP+ATM-B (J, 1)
A3=ATP+B (J, 2) / DY
A4=B (J, 3) - B (J, 2) * B (J, 5) - B (J, 1) * VHPP (J)
VH (J)=A3 / (A2-A1 * VH (J-1))
VHP (J)=(A4+A1 * VHP (J-1)) / (A2-A1 * VH (J-1))
200 CONTINUE
VHPP (JY)=VHPP (JY-1) + (B (JY, 5) + B (JY-1, 5)) / 2. * (Y (JY) - Y (JY-1))
FP (JY)=FPE
DO 250 JJ=1, JYM
J=JY-JJ
FP (J)=VH (J) * (FE (J+1) + VHEP (J+1)) - VHPP (J) + VHP (J)
250 CONTINUE
DO 300 JJ=1, JYM
J=JY-JJ
IF (ABS (FP (J)) .GT. 1.E-8) GO TO 301
JE=J
300 CONTINUE
301 CONTINUE
RETURN
END

```

(III-17)  
(III-19a)  
(III-19b)

(III-26)

Subroutine INTEG performs a simple trapazoidal quadrature.

Classification of Arguments

Inputs: JE, JE, Y, FP, FIRST.

Outputs: F.

```
SUBROUTINE INTEG (JE, JE, Y, FP, FIRST, F)
DIMENSION Y(JD), FP(JD), F(JD)
JEM=JE-1
FP2=FP(1)
F1=FIRST
F(1)=F1
DO 110 J=1, JEM
FP1=FP2
FP2=FP(J+1)
F1=F1+(Y(J+1)-Y(J))*(FP2+FP1)/2.
F(J+1)=F1
110 CONTINUE
IF (JE.GE.JD) RETURN
DO 120 J=JE, JD
F(J)=F(JE)
120 CONTINUE
RETURN
END
```

Subroutine FILE prints out the profiles and parameters at each x station.

Classification of Arguments

Inputs: LABEL, I, YY, F, FP, FPP, GP, GPP, D, DP, VH, VHP, VHPP,  
 TAU, VE, VEG, SHR, BH, PR, PRT, X, U, M, TURB, RW, VW,  
 SW, CW, RDT, DT, MT, HT, SF, CF, ST, STR, ID, JE, JY,  
 JD, JDIV.

Outputs: NONE.

```

SUBROUTINE FILE (LABEL, I, YY, F, FP, FPP, GP, GPP, D, DP,
1  VH, VHP, VHPP, TAU, VE, VEG, SHR, BH, PR, PRT,
2  X, U, M, TURB, RW, VW, SW, CW,
3  RDT, DT, MT, HT, SF, CF, ST, STR, ID, JE, JY, JD, JDIV)
REAL M, MT
DIMENSION YY(JD), BB(13), LABEL(18)
DIMENSION F(JD), FP(JD), FPP(JD), GP(JD), GPP(JD), D(JD), DP(JD)
DIMENSION VH(JD), VHP(JD), VHPP(JD), VE(JD), VEG(JD), TAU(JD)
DIMENSION X(ID), U(ID), M(ID), TURB(ID), RW(ID), VW(ID), SW(ID),
1  CW(ID)
DIMENSION DT(ID), MT(ID), HT(ID), SF(ID), RDT(ID)
DIMENSION CF(ID), ST(ID), STR(ID)
WRITE (6,10) (LABEL(K), K=1,18)
WRITE (6,11) X(I), U(I), M(I), RDT(I)
WRITE (6,12) TURB(I), RW(I), VW(I), SW(I), CW(I)
WRITE (6,13) DT(I), MT(I), HT(I), SF(I), CF(I), ST(I)
WRITE (6,14) BH, PR, PRT, SHR
WRITE (6,20)
DO 100 J=1, JE, JDIV
BB(1)=YY(J)
BB(2)=D(J)*(1.-FP(J))
BB(3)=F(J)
BB(4)=FP(J)
BB(5)=FPP(J)
BB(6)=D(J)
BB(7)=GP(J)
BB(8)=GPP(J)
BB(9)=TAU(J)
BB(10)=VE(J)
BB(11)=VH(J)
BB(12)=VHP(J)
BB(13)=DP(J)/D(J)*(1.-FP(J))
WRITE (6,21) J, (BB(K), K=1, 13)
100 CCNTINUE
WRITE (6,9)
RETURN
9  FORMAT (1H1)
10  FORMAT (1HC, 46X, 27HBOUNDARY LAYER PROFILES FOR //26X, 18A4//)
11  FORMAT (1HC, 33X, 3HX =, F8.3, 3X, 3HU =, F9.3, 3X, 3HM =, F6.2,
1  3X, 5HRT =, F9.2)
12  FORMAT (1HC, 23X, 6HTURE =, F5.3, 4X, 4HRW =, 1PE9.2, 4X,
1  4HWV =, F9.2, 3X, 4HSW =, E9.2, 3X, 4HCW =, E9.2)
13  FORMAT (1HC, 15X, 4HDT =, 1PE9.2, 1X,
1  4HMT =, F9.2, 1X, 4HHT =, F9.2, 1X, 4HSP =, E9.2, 1X,
2  4HCF =, F9.2, 1X, 4HST =, E9.2)
14  FORMAT (1HC, 31X, 4HHR =, 1PE9.2, 3X, 4HPP =, E9.2, 3X,
1  5HPRT =, E9.2, 3X, 5HSHR =, F5.2)
20  FORMAT (1HC, 4X, 1HJ, 6X, 2HYU, 7X, 1HU/U, 7X, 1HP, 8X, 2HFP,
1  7X, 3HPFP, 7X, 1HD, 8X, 2HGP, 6X, 3HGPP, 6X, 3HTAU,
2  7X, 2HVE, 8X, 2H
21  FORMAT (4X, I3, 1X, 4(1PE9.2), 1X, 3F9.2, 1X, 3E9.2, 3(1X, E9.2))
END
    
```

## V. PROGRAM OPERATION

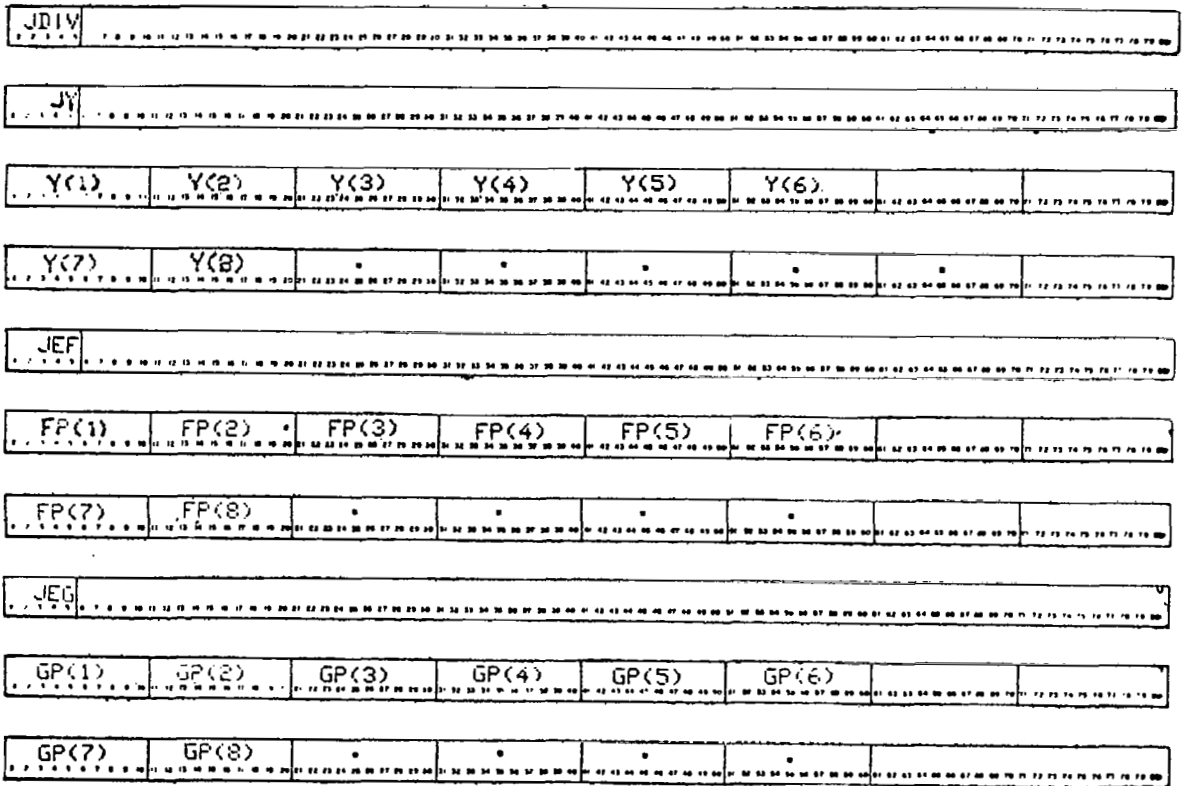
### Input

Just as the program itself falls into two parts, the input to the program is best considered in two parts. The first part is the choice of the method of initialization best suited to a specific problem. Here the decision is made on the basis of which method best represents reality. The second part of the input concerns the downstream calculation. There is considerably more latitude in the specification of how this is to be carried out.

The input to the initialization section begins with a title, written in the first 72 columns of the first card. This title is printed as a label on all of the output produced by the program

```
..... LABEL DESCRIBING CALCULATION .....
```

The first group of numerical inputs apply to the distribution of  $\eta$  points and the input  $f'(\eta)$  and  $g'(\eta)$  profiles. To save the effort on preparing a large number of input values, provision has been made in the program to subdivide the input values of  $\eta$ ,  $f'(\eta)$  and  $g'(\eta)$ . The number of subdivisions between each input value is specified by JDIV. The total number of  $\eta$  values which is to follow is JY. JY and JDIV must be such that the product of JDIV and JY is less than JD. Then the  $\eta$  values are listed 6 to a card. These are followed by JEF, defining the total number of profile values FP and the FP values themselves listed 6 to a card. Finally, JEG, the number of profile values of GP, and the GP values are specified, also 6 to a card.



Since the  $\eta$  step size is fixed, the input  $\eta$  spacing, when subdivided by JDIV, should be adequate to define a profile. In a wholly laminar calculation the  $\eta$  spacing need not vary appreciably across the layer but in a calculation with a turbulent portion, smaller spacing should be prescribed close to the wall than is specified further out, in order to resolve details both viscous and logarithmic in portions of the law of the wall region. The outer edge of the boundary layer in  $\eta$  coordinates will not move in or out appreciably as the calculations proceed downstream because  $\eta$  has been normalized with  $\delta^*$ . However, fineness of  $\eta$  spacing near the wall will be conditioned by the largest Reynolds number encountered in a calculation. A few sample calculations should provide the necessary experience. The samples of  $\eta$  distributions presented in these examples should cover most cases, however. Finally, for very small  $x$  step size, smaller  $\eta$  spacing will be required throughout the layer.

In the specification of the initial  $f'$  and  $g'$  profiles, the requirements differ greatly depending on whether the input profiles are to be used without change or are to be recalculated. If the input profiles are to be used as they are, some confidence in their compatibility with the initial pressure gradient is necessary. For a turbulent flow, the profiles must be well defined in the law of the wall region. If the profiles are known from experiments, for instance, and as is frequently the case, only the outer parts are known with confidence, then it is best to supply the required  $f'$  points close to the wall from some of the empirical "law of the wall". On the other hand, if the initial profile is to be recalculated to obtain a similarity solution, it may be a rough guess; the calculation of the similarity solutions converge strongly to profiles independent of the input profiles.

The next few cards are concerned with the method of initialization itself. The variety of situations for which the program has been implemented is given in the following outline, along with the appropriate sets of input cards for each. Their theoretical basis has been discussed in Section II.

The first parameter on the first card of each group, IOP, is the initialization option number as assigned in the following outline. The second parameter, MOP, designates the method of calculating the total enthalpy parameter. A table of possible values of MOP is given below. The third control parameter is DOP. It controls the interpretation of the input data. The table below describes the use of DOP. Last of all, the parameter IO must be specified. IO determines whether an axisymmetric flow will be calculated on the inside (IO = -1) or the outside (IO = 1) of the surface. For plane flow, IO need not be specified.



FLOW PROPERTIES		METHOD OF OBTAINING THE $g'(\eta)$ PROFILE
NOT VARIABLE	VARIABLE	
-1	1	$h^\circ$ assumed constant and equal to $h_e^\circ$ throughout the layer; $g'(\eta) = 0.0$ .
-2	2	$g'_w = GBC = [h_e^\circ - h_w(x)]/(h_e^\circ - h_r)$ is the wall boundary condition imposed on the energy equation.
-3	3	$g''_w = -(GBC)d_w/T_w = -S_{tr}d_w/T_w$ is the wall boundary condition imposed on the energy equation where $S_{tr} = R_L S_{tr} = lg_w/[\rho_e v_\infty (h_e^\circ - h_r)]$ for laminar similarity starting solutions and $S_{tr} = S_{tr} = g_w/[\rho_e U(h_e^\circ - h_r)]$ for all others.

TABLE 1a. ALTERNATIVE VALUES OF MOP

The index IBC, the absolute value of MOP, also appears explicitly in the program.

INTERPRETATION OF INPUT $U_{in}(I)$		INTERPRETATION OF INPUT
$U_{in}(I) \xrightarrow{*} M(I)$	$U_{in} \xrightarrow{*} U(I)$	$f'_{in}(\eta)$ PROFILE
-1	1	$f'_{in}(\eta) \xrightarrow{*} (U - u)/U$ $V_{w,in} = V_w$
-2	2	$f'_{in}(\eta) \xrightarrow{*} (\rho_e U - \rho u)/(\rho_e U)$ $V_{w,in} = (\rho_w/\rho_e)V_w$

TABLE 1b. ALTERNATIVE VALUES OF DOP

\*Note that the interchanges marked with an asterisc take place at the beginning of the program and thereafter  $U(I)$  and  $f'(\eta)$  have their conventional meanings, whereas  $VW(I)$  represents  $(\rho_w/\rho_e)V_w$  throughout the calculation for DOP =  $\pm 2$ .





Option 7, initial  $\delta^*$ ,  $R\delta^*$ , and  $(U_x\delta^*/U)$  are known.

7	MOP	DOP	ID																
MR	DT(1)	RDT(1)	P	T0	BH														
X(1)	U(1)	1.0	GEC(1)	RW(1)	VW(1)	SW(1)	CW(1)												

Only in Option 4 is the calculation actually starting from the beginning of the boundary layer growth. In this case, the position  $X(I)$  corresponds to this initial point where either  $DT$  or  $U$  should be zero and the similarity laws are used to provide values at  $X(2)$ . Therefore, to calculate a plane stagnation point flow ( $B = 1.0$ ), for example,  $U(1)$  must be 0.0. Similarly, a Blasius flow ( $B = 0.0$ ),  $DT(1)$  must be 0.0.  $RW(1)$  may be either finite or zero depending on the geometry. For the flow starting at the apex of a cone,  $RW(1)$  will be zero but  $RW(2)$  will be nonzero. On the other hand, a flat plate flow will have all  $RW$  values equal to zero, as described below. Also, in Option 4,  $VW(1)$  must be zero since transpiration is not compatible with the boundary layer assumptions for  $U^2\delta^* = 0$ .

Having initialized the calculation, it remains to specify the information required for the downstream calculations. This is accomplished with a set of cards each containing the parameters related to an  $X$  station. The first two parameters,  $X$  and  $U$  must appear on each card. The remainder need not be specified unless they apply in a particular case.

X(I)	U(I)	TURB(I)	GEC(I)	RW(I)	VW(I)	SW(I)	CW(I)												
X(I+1)	U(I+1)	TURB(I+1)	GEC(I+1)	RW(I+1)	VW(I+1)	SW(I+1)	CW(I+1)												
.	.	.	.	.	.	.	.												
.	.	.	.	.	.	.	.												
-10000.0																			

The sequence of X values on successive cards define the X spacing at which calculations will be performed. As in the case of the Y spacing, there is no mechanism for altering the X step size to maintain accuracy. The reason for this is that there is generally no need for it. The numerical method itself is sufficiently forgiving to be accurate over a wide range of step size. The controlling consideration then is to represent the mainstream velocity distribution realistically. But since this is known, the X steps can be chosen in advance. In the case of layers near equilibrium, steps of the order of many hundreds of displacement thicknesses are possible. On the other hand, if the mainstream velocity changes rapidly, steps may be small.

The values of U, corresponding to each X, define the freestream velocity (or Mach number if DOP is negative). U may be in either dimensional or nondimensional form since it appears only as a ratio in the calculations.

The third quantity that can be specified is TURB, which indicates whether the flow is laminar (TURB = 0.0) or turbulent (TURB = 1.0). If the flow is laminar, no empirical content is necessary since the laminar boundary layer equations are complete. However, if the flow is turbulent, a semi-empirical effective viscosity assumption is necessary to close the equations. The form of this assumption is given in Section I and the basis for the assumption is discussed in greater detail in Reference [2]. TURB also has another function. By changing TURB from 0.0 to 1.0, either abruptly or gradually over the distance of several X stations, the effect of transition can be simulated. There is no mechanism within the program to decide when or how this should be done. This information must be supplied by the user, either from consideration of the boundary conditions or from previous calculation attempts (see, for instance, [11], Chapters XVI and XVII).

GBC is the wall boundary condition on the energy equation. Various interpretations of GBC are made according to the value of the parameter MOP. These are described in Table 1.

RW is the radius of the wall in a flow over an axisymmetric body. The units of RW must be the same as those of X. For a planar flow RW may be left blank, which is treated as an infinite radius of curvature.

It is possible to calculate flows with transpiration or aspiration by specifying  $VW = v_w(x)$ . VW is positive for transpiration and negative for aspiration.

Another boundary condition that can be specified is the wall roughness. This is done in the form of average roughness size,  $SW = s_w$ . Again the units of SW must be the same as those of X.

The longitudinal radius of curvature,  $CW = c_w$ , in the same units as X, is the last boundary condition which can be prescribed.

Finally, there are several constants which for clarity have not been made data inputs, but are set in data statements as the beginning of the program. The first of these concern the properties of the fluid. They are the specific heat ratio of the fluid,  $SHR = C_p/C_v$ , the constant,  $S_c$ , in the Sutherland viscosity relation and the molecular and turbulent Prandtl numbers,  $P_r$  and  $P_{rt}$ .

In addition, there are some constants which are set to suit the particular computer used. The first two of these are JD and ID, which specify the maximum number of calculation points perpendicular to and parallel to the wall, respectively. The values given in the listing (JD = 300, ID = 60) are considerably larger than necessary in most practical calculations. It is possible that in some cases they may need to be made larger or smaller depending on the storage capacity of the computer to be used. This may be done by changing the values in the data statement and also by specifying consistent values in the dimension statements both of which are at the beginning of the Main Program.

## Output

The primary output from the calculations is a list of the calculated profiles and parameters that is printed out with the subroutine \$FILE for each X station (see, for example, Table 2c). This output form gives the principle input and output parameters at the top. Below these are the various profiles as functions of J and  $y/\delta^*$ . The profiles are identified with symbols which are for the most part identical and variable names used in the program (see Notation). The exception is U/U which represents  $u/U$ . The last three columns are not used but are included for the convenience of the user so that other profiles may be printed out.

The output of the calculation begins with a print-out of the input profiles and other related profiles which have been calculated from it with \$FILE. The next page begins with a list of the input parameters for reference. These are identified and are, therefore, self-explanatory. Below this, in the case that the initial profile is recalculated, is a list of significant parameters for each iteration indicating, among other things, the rate of convergence.

There are primary lines of parameters of two types. One records a calculation by the momentum equation and the other records a calculation by the energy equation. These different lines may be identified by the letters F and G, respectively, which are printed on the left-hand margin of the list. In this list of significant parameters, as in the case of \$FILE, the parameters are identified with the same symbols as were used in the program. The first two are indices of key points on the profiles which are shown in Figure 3 in Section IV. The next five parameters on the F line are related to the profile as a whole. FJE is  $F(JE)$ , the integral

$$f(\infty) = \int_0^{\infty} f'(\eta) d\eta, \quad (V-1)$$

and FPPW is  $F''(0)$ . The three profile parameters on the G line are GPW, GPPW and DW which are  $g'(0)$ ,  $g''(0)$  and  $d(0)$ , respectively. Finally, the recalculated profiles are printed out with  $\phi$ FILE and this signifies the end of the initialization.

The output of the calculation moving downstream consists of two parts. The first is the list of significant parameters for each iteration as in the case of the recalculated profile. This time, however, an indication of the accuracy of the numerical integration along the wall is printed out. This is done in the form of two pairs of numbers, for the momentum and energy equations, respectively, one on either side of each equal sign which correspond to the left and right-hand sides of equations (II-21) and (II-23) in Section II. Closer agreement between each pair of numbers indicates more accurate integration.

The second part of the output at each X station is the print-out of the profiles and parameters with \$FILE.

Finally, at the end of the calculation for the entire series of X stations, a summary of the important integral parameters of the flow is printed out for convenience.



## Illustrative Examples

Two boundary layer calculations have been performed to demonstrate some of the capabilities of the program.

The first calculation has been made to compare with data measured by Moore and Harkness [18]. These measurements are for an adiabatic, compressible turbulent flow on a flat plate at a Mach number of 2.669. A listing of the necessary input cards for this case is given in Table 2a. A sample listing of the various calculated profiles is shown in Table 2c preceded by a print-out of the iterations which produced it. Finally, the summary of integral parameters is given in Table 2d.

A comparison between the calculations and the experimental data for the velocity profile is shown in Figure 5. In addition, direct measurement of the skin friction was made which provides an additional basis for comparison. The experimental value of  $C_f$  was found to be 0.000862 whereas, the calculated value is 0.000883.

The other example calculation is for a constant property, turbulent flow with heat transfer which was one of a series measured by Moretti and Kays [19]. The freestream velocity distribution and wall temperature distribution for this case are shown in Figure 6. The interesting feature of this flow is the sequence of step changes in wall temperature which produces a complex Stanton number distribution.

The input data is listed in Table 3a and the parameter and profile listing for a sample location is given in Tables 3b and 3c. Table 3d provides the listing of parameters for the entire flow and Figure 6 shows the good agreement between the Stanton number calculations and the data.

## Identification of Malfunctions

The calculations of the examples above all proceeded smoothly. However, this may not always be the case. To aid in the diagnosis of problems that may be encountered, some of the more common difficulties are discussed here.

MOORE AND HARKNESS

3					
6.9					
0.0	0.000002	0.000005	0.00001	0.00002	0.00005
0.00001	0.00002	0.00005	0.0001	0.00015	0.0002
0.00025	0.0003	0.00035	0.0004	0.0005	0.0006
0.0008	0.0010	0.0020	0.0030	0.0040	0.0050
0.1	0.2	0.3	0.4	0.5	0.6
0.7	0.8	0.9	1.0	1.2	1.4
1.6	1.8	2.0	2.5	3.0	3.5
4.0	4.5	5.0	5.5	6.0	6.5
7.0	7.5	8.0	8.5	9.0	9.5
10.0	11.0	12.0	13.0	14.0	16.0
18.0	20.0	22.0	24.0	26.0	28.0
30.0	35.0	40.0			
45					
1.0	0.9996	0.9990	0.998	0.996	0.990
0.980	0.960	0.900	0.843	0.823	0.811
0.801	0.793	0.787	0.781	0.771	0.762
0.749	0.738	0.702	0.680	0.663	0.649
0.605	0.555	0.523	0.498	0.478	0.462
0.445	0.423	0.411	0.394	0.358	0.322
0.266	0.251	0.218	0.143	0.0856	0.0447
0.0190	0.00467	0.0			
6					
0.0	0.0	0.0	0.0	0.0	0.0
6	-2				
2.669	0.876	2600000.0	0.0	305.0	1.0
0.0	2.669	1.0	0.0		
10.0	2.669	1.0	0.0		
20.0	2.669	1.0	0.0		
30.0	2.669	1.0	0.0		
40.0	2.669	1.0	0.0		
50.0	2.669	1.0	0.0		
60.0	2.669	1.0	0.0		
80.0	2.669	1.0	0.0		
-10000.0					

Table 2a. Moore and Harkness  
Input Data





PRINCIPAL BOUNDARY LAYER PARAMETERS FOR  
MOORE AND HARKNESS

X	DT	MT	HT	SF	CF	ST	GPW	RDT	U	M	TURB	RW	VW	SW	CW
0.0	0.876000	0.205041	-0.00039	4.272	0.00091	0.0	0.01356	2690900.	1.000	2.669	1.000	0.0	0.0	0.0	0.0
10.00000	0.894107	0.209625	-0.00040	4.265	0.00091	0.0	0.01351	2653739.	1.000	2.669	1.000	0.0	0.0	0.0	0.0
20.00000	0.917529	0.214149	-0.00040	4.285	0.00091	0.0	0.01347	2723254.	1.000	2.669	1.000	0.0	0.0	0.0	0.0
30.00000	0.932355	0.218663	-0.00041	4.264	0.00090	0.0	0.01345	2767258.	1.000	2.669	1.000	0.0	0.0	0.0	0.0
40.00000	0.949425	0.223149	-0.00041	4.255	0.00089	0.0	0.01343	2817920.	1.000	2.669	1.000	0.0	0.0	0.0	0.0
50.00000	0.973165	0.227619	-0.00042	4.275	0.00089	0.0	0.01340	2888376.	1.000	2.669	1.000	0.0	0.0	0.0	0.0
60.00000	0.989569	0.232075	-0.00042	4.264	0.00089	0.0	0.01338	2937060.	1.000	2.669	1.000	0.0	0.0	0.0	0.0
80.00000	1.028622	0.240931	-0.00043	4.269	0.00088	0.0	0.01334	3052965.	1.000	2.669	1.000	0.0	0.0	0.0	0.0

Table 2d. Moore and Harkness  
Summary of Important Input and Output  
Parameters for Entire Calculation

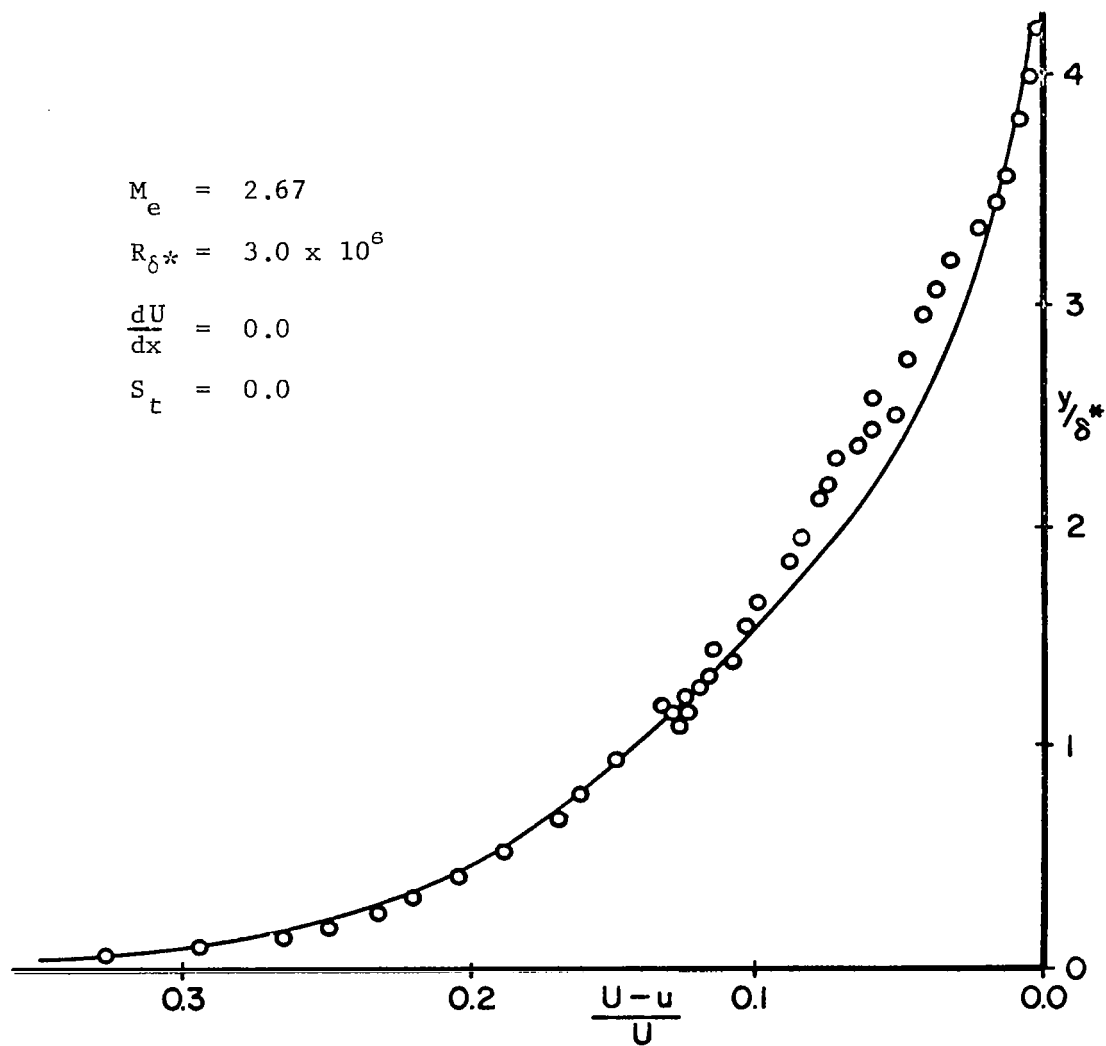


Figure 5. Comparison Between a Velocity Profile Measured by Moore and Harkness [18] and the Calculated Profile Shown With an Unbroken Line. The Calculated  $C_f$  was 0.000873 Which Compares Well With the Experimental Value of 0.000862.

MORETTI AND KAYS, CASE 24

3					
5.1					
00.0	0.002	0.005	0.01	0.02	0.05
0.1	0.2	0.3	0.4	0.5	0.6
0.7	0.8	0.9	1.0	1.2	1.4
1.1	1.8	2.0	2.5	3.0	3.5
1.6	4.5	5.0	5.5	6.0	6.5
4.0	7.5	8.0	8.5	9.0	9.5
7.0	11.0	12.0	13.0	14.0	16.0
10.0	20.0	22.0	24.0	26.0	28.0
18.0	35.0	40.0			
30.0					
33.0					
1.0	0.992	0.981	0.962	0.924	0.813
0.6	0.506	0.449	0.418	0.393	0.373
0.3	0.340	0.326	0.314	0.291	0.269
0.2	0.227	0.207	0.160	0.118	0.0833
0.5	0.0350	0.0207	0.0114	0.00589	0.00283
0.5	0.00052	0.0			
0.0127					
30					
0.184	0.182	0.180	0.176	0.168	0.145
0.11	0.0738	0.0596	0.0519	0.0461	0.0415
0.0377	0.0345	0.0319	0.0295	0.0251	0.0212
0.0177	0.0147	0.0120	0.00705	0.00392	0.00206
0.00103	0.000491	0.000223	0.0000942	0.0000406	0.0000163
6	-2	1			
0.0	0.05	2000.0	0.0	300.0	1.0
12.7	0.300	1.0	0.212		
15.3	0.3025	1.0	0.214		
15.8	0.3033	1.0	0.214		
16.8	0.3048	1.0	0.214		
19.0	0.3082	1.0	0.215		
20.0	0.3100	1.0	0.215		
21.0	0.3129	1.0	0.239		
21.9	0.3170	1.0	0.281		
23.0	0.3210	1.0	0.359		
24.1	0.3250	1.0	0.549		
25.1	0.330	1.0	0.962		
26.2	0.339	1.0	0.980		
27.1	0.348	1.0	0.999		
28.1	0.357	1.0	0.999		
29.1	0.363	1.0	0.937		
30.2	0.370	1.0	0.965		
31.2	0.377	1.0	0.691		
32.3	0.384	1.0	0.521		
33.2	0.391	1.0	0.448		
34.3	0.398	1.0	0.415		
35.4	0.406	1.0	0.453		
36.4	0.414	1.0	0.583		
37.6	0.422	1.0	0.882		
38.6	0.427	1.0	0.945		
39.5	0.433	1.0	0.960		
40.5	0.438	1.0	0.966		
41.7	0.444	1.0	0.934		
42.6	0.463	1.0	0.934		
43.6	0.473	1.0	0.677		
44.7	0.483	1.0	0.527		
45.7	0.496	1.0	0.432		
46.7	0.509	1.0	0.399		
47.7	0.520	1.0	0.392		
48.7	0.531	1.0	0.476		

Table 3a. Moretti and Kays, Case 24  
Input Data

4	0	1	0
5	0.542	1	0.754
5	0.561	1	0.799
5	0.580	1	0.847
5	0.599	1	0.840
5	0.620	1	0.846
5	0.640	1	0.823
5	0.660	1	0.568
5	0.680	1	0.422
5	0.702	1	0.357
5	0.725	1	0.335
6	0.747	1	0.347
6	0.770	1	0.446
6	0.800	1	0.699
6	0.830	1	0.751
6	0.860	1	0.757
6	0.890	1	0.756
6	0.920	1	0.724
6	0.940	1	0.748
6	0.960	1	0.748
6	0.974	1	0.720
7	0.980	1	0.715
7	0.999	1	0.690
7	1.000	1	0.704
7	1.000	1	0.718
7	1.000	1	0.519
10000.0			

Table 3a. (cont.)



INPUT VARIABLES FOR

MORETTI AND KAYS, CASE 24

X = 7.45E 01 U = 1.00E 00 M = 0.0

TURB = 1.0 GBC = 5.19E-01 PW = 0.0

VW = 0.0

SW = 0.0

CW = 0.0

VALUES OF IMPORTANT VARIABLES FOR EACH ITERATION

P	JK	JEP	FJE	FPPW	DT	DIXM	PM	QM	RM
G		JEG	GPW	GPPW	LW				
P	46	135	1.00E 00	-8.85E 00	4.04E-02	2.30E-03	9.35E-09	2.30E-03	0.0
P	46	135	1.00E 00	-8.82E 00	4.04E-02	2.30E-03	9.35E-09	2.30E-03	0.0
G		137	5.19E-01	-1.62E 00	1.00E 00				

INTEGRALS OF MOMENTUM AND ENERGY EQUATIONS

MOMENTUM  
1.0581 = 1.0580

ENERGY  
1.6156 = 1.6175

Table 3b. Moretti and Kays, Case 24  
Significant Parameters for Each Iteration at X = 74.5



PRINCIPAL BOUNDARY LAYER PARAMETERS FOR  
MORETTI AND KAYS, CASE 24

X	DT	HT	HT	SF	CF	ST	GPW	RDT	U	M	TURB	RW	VW	SW	CV
12.70000	0.050000	0.034340	0.008031	1.456	0.00384	0.00302	0.21200	2000.	0.300	0.0	1.000	0.0	0.0	0.0	0.0
15.30000	0.054906	0.038372	0.009244	1.431	0.00388	0.00210	0.21400	2215.	0.302	0.0	1.000	0.0	0.0	0.0	0.0
15.80000	0.055842	0.038988	0.009441	1.432	0.00386	0.00207	0.21400	2258.	0.303	0.0	1.000	0.0	0.0	0.0	0.0
16.79999	0.057494	0.040248	0.009836	1.428	0.00386	0.00206	0.21400	2337.	0.305	0.0	1.000	0.0	0.0	0.0	0.0
19.00000	0.060895	0.042912	0.010703	1.419	0.00384	0.00203	0.21500	2502.	0.308	0.0	1.000	0.0	0.0	0.0	0.0
20.00000	0.062026	0.043974	0.011098	1.411	0.00385	0.00201	0.21500	2564.	0.310	0.0	1.000	0.0	0.0	0.0	0.0
21.00000	0.062192	0.044513	0.011522	1.397	0.00391	0.00223	0.23900	2595.	0.313	0.0	1.000	0.0	0.0	0.0	0.0
21.89999	0.061771	0.044307	0.011863	1.394	0.00393	0.00246	0.28100	2611.	0.317	0.0	1.000	0.0	0.0	0.0	0.0
23.00000	0.061780	0.044591	0.012649	1.385	0.00396	0.00268	0.35900	2644.	0.321	0.0	1.000	0.0	0.0	0.0	0.0
24.09999	0.061980	0.044906	0.014065	1.380	0.00399	0.00304	0.54900	2686.	0.325	0.0	1.000	0.0	0.0	0.0	0.0
25.09999	0.060970	0.044621	0.016520	1.366	0.00408	0.00336	0.96200	2683.	0.330	0.0	1.000	0.0	0.0	0.0	0.0
26.20000	0.058080	0.042935	0.019001	1.353	0.00421	0.00281	0.98000	2625.	0.339	0.0	1.000	0.0	0.0	0.0	0.0
27.09999	0.055431	0.041149	0.020797	1.347	0.00429	0.00274	0.99900	2572.	0.348	0.0	1.000	0.0	0.0	0.0	0.0
28.09999	0.053502	0.039828	0.022750	1.343	0.00429	0.00264	0.99900	2547.	0.357	0.0	1.000	0.0	0.0	0.0	0.0
29.09999	0.053401	0.039759	0.024898	1.343	0.00426	0.00244	0.93700	2585.	0.363	0.0	1.000	0.0	0.0	0.0	0.0
30.20000	0.053086	0.039564	0.027113	1.342	0.00423	0.00248	0.96500	2619.	0.370	0.0	1.000	0.0	0.0	0.0	0.0
31.20000	0.052510	0.039206	0.028106	1.339	0.00421	0.00163	0.69100	2639.	0.377	0.0	1.000	0.0	0.0	0.0	0.0
32.29999	0.052331	0.039124	0.028760	1.338	0.00421	0.00131	0.52100	2679.	0.384	0.0	1.000	0.0	0.0	0.0	0.0
33.20000	0.051730	0.038662	0.028753	1.338	0.00419	0.00121	0.44800	2697.	0.391	0.0	1.000	0.0	0.0	0.0	0.0
34.29999	0.051712	0.038680	0.028970	1.337	0.00417	0.00127	0.41500	2744.	0.398	0.0	1.000	0.0	0.0	0.0	0.0
35.39999	0.051371	0.038413	0.029185	1.337	0.00417	0.00166	0.45300	2781.	0.406	0.0	1.000	0.0	0.0	0.0	0.0
36.39999	0.050677	0.038001	0.029590	1.334	0.00415	0.00220	0.58300	2797.	0.414	0.0	1.000	0.0	0.0	0.0	0.0
37.59999	0.050849	0.038046	0.031259	1.337	0.00409	0.00265	0.88200	2861.	0.422	0.0	1.000	0.0	0.0	0.0	0.0
38.59999	0.051508	0.038590	0.033238	1.335	0.00407	0.00243	0.94500	2933.	0.427	0.0	1.000	0.0	0.0	0.0	0.0
39.50000	0.051635	0.038607	0.034622	1.337	0.00402	0.00231	0.96600	2981.	0.433	0.0	1.000	0.0	0.0	0.0	0.0
40.50000	0.052227	0.039124	0.036437	1.335	0.00399	0.00224	0.96600	3050.	0.438	0.0	1.000	0.0	0.0	0.0	0.0
41.70000	0.052758	0.039850	0.039956	1.324	0.00417	0.00213	0.93400	3123.	0.444	0.0	1.000	0.0	0.0	0.0	0.0
42.59999	0.047757	0.036375	0.038755	1.313	0.00418	0.00207	0.93400	2948.	0.463	0.0	1.000	0.0	0.0	0.0	0.0
43.59999	0.047535	0.035942	0.039392	1.323	0.00423	0.00134	0.67700	2998.	0.473	0.0	1.000	0.0	0.0	0.0	0.0
44.70000	0.047642	0.035780	0.039867	1.315	0.00418	0.00101	0.52700	3029.	0.483	0.0	1.000	0.0	0.0	0.0	0.0
45.70000	0.045615	0.034759	0.039173	1.312	0.00419	0.00071	0.43200	3017.	0.496	0.0	1.000	0.0	0.0	0.0	0.0
46.70000	0.044519	0.033905	0.038363	1.313	0.00418	0.00077	0.39900	3021.	0.509	0.0	1.000	0.0	0.0	0.0	0.0
47.70000	0.044154	0.033603	0.037949	1.314	0.00415	0.00089	0.39200	3061.	0.520	0.0	1.000	0.0	0.0	0.0	0.0

SZ

Table 3d. Moretti and Kays, Case 24  
Summary of Important Input and Output  
Parameters for Entire Calculation

48.70000	0.043772	0.033343	0.037672	1.313	0.00411	0.00152	0.47600	3099.	0.531	0.0	1.000	0.0	0.0	0.0	0.0
49.89999	0.044101	0.033573	0.039220	1.314	0.00413	0.00230	0.75400	3187.	0.542	0.0	1.000	0.0	0.0	0.0	0.0
51.00000	0.041889	0.032092	0.039340	1.305	0.00416	0.00206	0.79900	3133.	0.561	0.0	1.000	0.0	0.0	0.0	0.0
52.00000	0.040121	0.030720	0.039455	1.306	0.00420	0.00209	0.84700	3103.	0.580	0.0	1.000	0.0	0.0	0.0	0.0
53.09999	0.038863	0.029839	0.040389	1.302	0.00425	0.00197	0.84000	3104.	0.599	0.0	1.000	0.0	0.0	0.0	0.0
54.00000	0.036996	0.028418	0.040085	1.302	0.00424	0.00194	0.84600	3058.	0.620	0.0	1.000	0.0	0.0	0.0	0.0
55.09999	0.036223	0.027828	0.040898	1.302	0.00426	0.00185	0.82300	3091.	0.640	0.0	1.000	0.0	0.0	0.0	0.0
56.00000	0.035058	0.026944	0.040275	1.301	0.00422	0.00086	0.56800	3085.	0.660	0.0	1.000	0.0	0.0	0.0	0.0
57.00000	0.034401	0.026427	0.039590	1.302	0.00421	0.00039	0.42200	3119.	0.680	0.0	1.000	0.0	0.0	0.0	0.0
58.00000	0.033546	0.025773	0.038438	1.302	0.00417	0.00023	0.35700	3140.	0.702	0.0	1.000	0.0	0.0	0.0	0.0
59.09999	0.032994	0.025354	0.037536	1.301	0.00416	0.00032	0.33500	3189.	0.725	0.0	1.000	0.0	0.0	0.0	0.0
60.00000	0.032248	0.024738	0.036411	1.304	0.00412	0.00060	0.34700	3212.	0.747	0.0	1.000	0.0	0.0	0.0	0.0
61.09999	0.032040	0.024544	0.036042	1.305	0.00410	0.00134	0.44600	3289.	0.770	0.0	1.000	0.0	0.0	0.0	0.0
62.29999	0.031186	0.023935	0.036019	1.303	0.00408	0.00206	0.69900	3326.	0.800	0.0	1.000	0.0	0.0	0.0	0.0
63.39999	0.030339	0.023334	0.036510	1.300	0.00413	0.00190	0.75100	3357.	0.830	0.0	1.000	0.0	0.0	0.0	0.0
64.20000	0.029008	0.022291	0.035894	1.301	0.00411	0.00182	0.75700	3326.	0.860	0.0	1.000	0.0	0.0	0.0	0.0
65.29999	0.028749	0.022054	0.036412	1.304	0.00409	0.00175	0.75600	3411.	0.890	0.0	1.000	0.0	0.0	0.0	0.0
66.29999	0.028171	0.021664	0.036072	1.300	0.00399	0.00161	0.72400	3455.	0.920	0.0	1.000	0.0	0.0	0.0	0.0
67.39999	0.029259	0.022300	0.037091	1.312	0.00392	0.00167	0.74800	3667.	0.940	0.0	1.000	0.0	0.0	0.0	0.0
68.29999	0.029475	0.022467	0.037177	1.312	0.00381	0.00160	0.74800	3773.	0.960	0.0	1.000	0.0	0.0	0.0	0.0
69.39999	0.030992	0.023430	0.037859	1.323	0.00369	0.00150	0.72000	4025.	0.974	0.0	1.000	0.0	0.0	0.0	0.0
70.39999	0.032800	0.024785	0.039235	1.323	0.00362	0.00149	0.71500	4286.	0.980	0.0	1.000	0.0	0.0	0.0	0.0
71.50000	0.033305	0.025123	0.038847	1.326	0.00352	0.00140	0.69000	4436.	0.999	0.0	1.000	0.0	0.0	0.0	0.0
72.59999	0.036050	0.026964	0.040218	1.337	0.00343	0.00146	0.70400	4807.	1.000	0.0	1.000	0.0	0.0	0.0	0.0
73.50000	0.038094	0.028487	0.041246	1.337	0.00334	0.00147	0.71800	5079.	1.000	0.0	1.000	0.0	0.0	0.0	0.0
74.50000	0.040396	0.030139	0.041888	1.340	0.00328	0.00074	0.51900	5386.	1.000	0.0	1.000	0.0	0.0	0.0	0.0

Table 3d. (cont.)

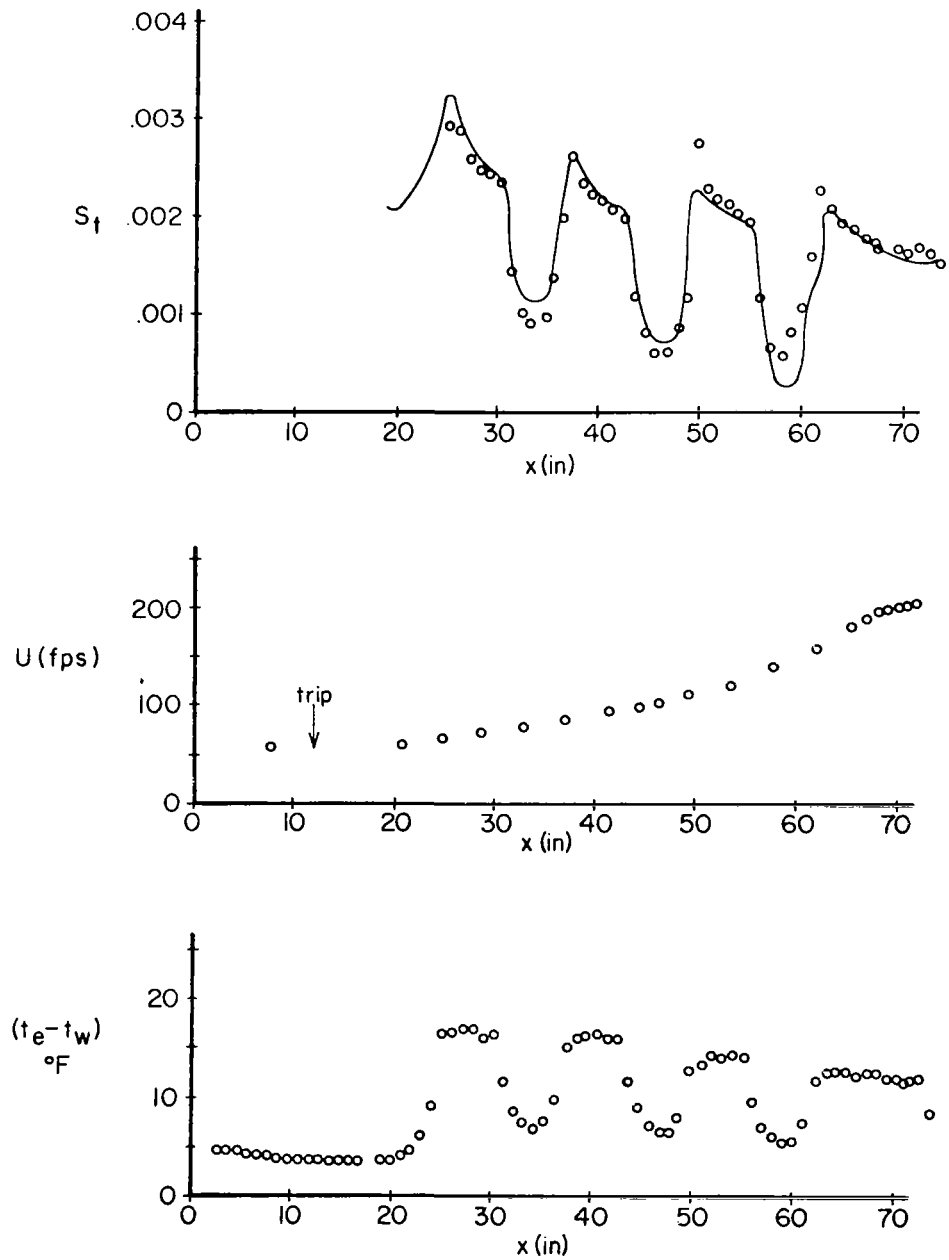


Figure 6. Comparison Between a Stanton Number Distribution Measured by Moretti and Kays [19] on a Cooled Flat Plate, and the Calculated Stanton Number Distribution Shown with an Unbroken Line. Also Shown are the Experimental Velocity Distribution and Wall Temperature Distribution Which Were Used for the Calculations.

The most common of these is simply that the solution does not converge. Indications that this has happened appear in the numbers printed out during the sequence of iterations. To begin with, FJE should be between 0.995 and 1.005. Also, FPPW and GPPW or GPW should have changed by less than 1/2% between the last two iterations for satisfactory convergence. Lack of convergence may result from a number of causes some of which will be described below.

The other important pattern of calculation failure is unjustified separation. This can be recognized by the fact that FPPW becomes positive, indicating a negative wall shear stress, and/or FJE becomes negative. Unjustified separation frequently occurs when the boundary layer is near actual separation. If one iteration behaves as if the separation point has been overstepped, then it is difficult for the calculation to recover.

Both of these malfunctions usually can be traced either to an actual error in the input data or to a poor choice of the X step size. In the latter case, the step size is too large if the shape factor is changing by more than about 5%. On the other hand, if the numbers on either side of the equal sign representing the INTEGRALS OF MOMENTUM AND ENERGY EQUATIONS are very close to 1.0000, then, if possible, the step size should be made larger for efficiency.

Other possible causes may be choices of boundary conditions which are incompatible with the assumptions used to derive the basic boundary layer equations. For example, the program will not calculate a boundary layer with a step change in freestream velocity or transpiration with  $v_w/U$  near 0.1. A radius of curvature in axial flow which is smaller than the boundary layer thickness may also give trouble, and very large roughness elements of the order of  $s_w/\delta^* = .1$  will not work for obvious reasons.

## REFERENCES

- [1] Herring, H.J. and Mellor, G.L., A Computer Program to Calculate Incompressible Laminar and Turbulent Boundary Layer Development, NASA CR-1564, (1970).
- [2] Herring, H.J. and Mellor, G.L., A Method of Calculating Compressible Turbulent Boundary Layers, NASA CR-1144 (1968).
- [3] Mellor, G.L. and Herring, H.J., Two Methods of Calculating Turbulent Boundary Layer Behavior Based on Numerical Solutions of the Equations of Motion. Proceedings - Conference on Computation of Turbulent Boundary Layer Prediction, Stanford University (1968).
- [4] Mellor, G.L. and Gibson, D.M., Equilibrium Turbulent Boundary Layers, J. Fluid Mech., Vol. 24, part 2, pp. 225-253 (1966).
- [5] Mellor, G.L., The Effects of Pressure Gradients on Turbulent Flow Near a Smooth Wall, J. Fluid Mech., Vol. 24, part 2, pp. 225-274 (1966).
- [6] Mellor, G.L., Incompressible, Turbulent Boundary Layers with Arbitrary Pressure Gradients and Divergent or Convergent Cross Flows, AIAA J., Vol. 5, no. 9, pp. 1570-1579 (1967).
- [7] Bradshaw, P., The Analogy Between Streamline Curvature and Buoyancy in Turbulent Shear Flow, J. Fluid Mech., Vol. 36, part 1, pp. 177-191 (1969).
- [8] Probstein, R.F. and Elliott, D., The Transverse Curvature Effect in Compressible Axially Symmetric Laminar Boundary Layer Flow, J. Aero. Sci. 23, pp. 208-224, 236 (1956).
- [9] Coles, D., The Law of the Wake in the Turbulent Boundary Layer, J. Fluid Mech., part 1, pp. 191-226 (1956).
- [10] Clauser, F., The Turbulent Boundary Layer, Advances in Applied Mechanics, Vol. IV, Academic Press, New York (1956).
- [11] Schlichting, H., Boundary Layer Theory, McGraw Hill, 4th Edition (1960).
- [12] Rosenhead, L., Laminar Boundary Layers, Oxford University Press (1963).
- [13] Crank, J. and Nicholson, P., A Practical Method for Numerical Integration of Solutions of Partial Differential Equations of Heat-Conduction Type. Proceedings - Cambridge Philos. Soc., Vol. 43, p. 50 (1947).

- [14] Richtmyer, R.D. and Morton, K.W., Difference Methods for Initial-Value Problems, Interscience Publishers, 2nd Edition (1967).
- [15] Nikuradse, J., Laws of Flow in Rough Pipes, NACA TM 1292 (1950).
- [16] So, R.M.C. and Mellor, G.L., An Experimental Investigation of Turbulent Boundary Layers Along Curved Surfaces, NASA CR-1940, (1971).
- [17] Mellor, G.L. and Herring, H.J., A Study of Turbulent Boundary Layer Models Part II, Mean Turbulent Field Closure, Sandia Corporation Report SC-CR-70-6125B, (1971).
- [18] Moore, D.R. and Harkness, J., Experimental Investigation of the Compressible Turbulent Boundary Layer at Very High Reynolds Numbers, Ling-Tempso-Vought, Research Center Report O-7100/4R-9, (1964).
- [19] Moretti, P.M. and Kays, W.M., Heat Transfer to a Turbulent Boundary Layer with Varying Freestream Velocity and Varying Surface Temperature - An Experimental Study, Int. J. Heat Mass Transfer, VIII, pp. 1187-1202 (1965).